Topological and Multipolar Magnets and Spintronics

Satoru Nakatsuji

Dept. of Physics, University of Tokyo
Institute for Solid State Physics (ISSP), University of Tokyo
Institute of Quantum Matters (IQM), Johns Hopkins University

Plan

- Multipole Physics on Correlated Electron Systems
- Topological States in Magnetic Systems
- Physics of Antiferromagnetic Weyl Semimetals
- Physics of Multipolar Kondo Lattice Systems

Lecture 4

- Multipole Physics on Correlated Electron Systems
- Topological States in Magnetic Systems
- Physics of Magnetic Weyl Semimetals
- Physics of Multipolar Kondo Lattice Systems

A pair of Weyl points

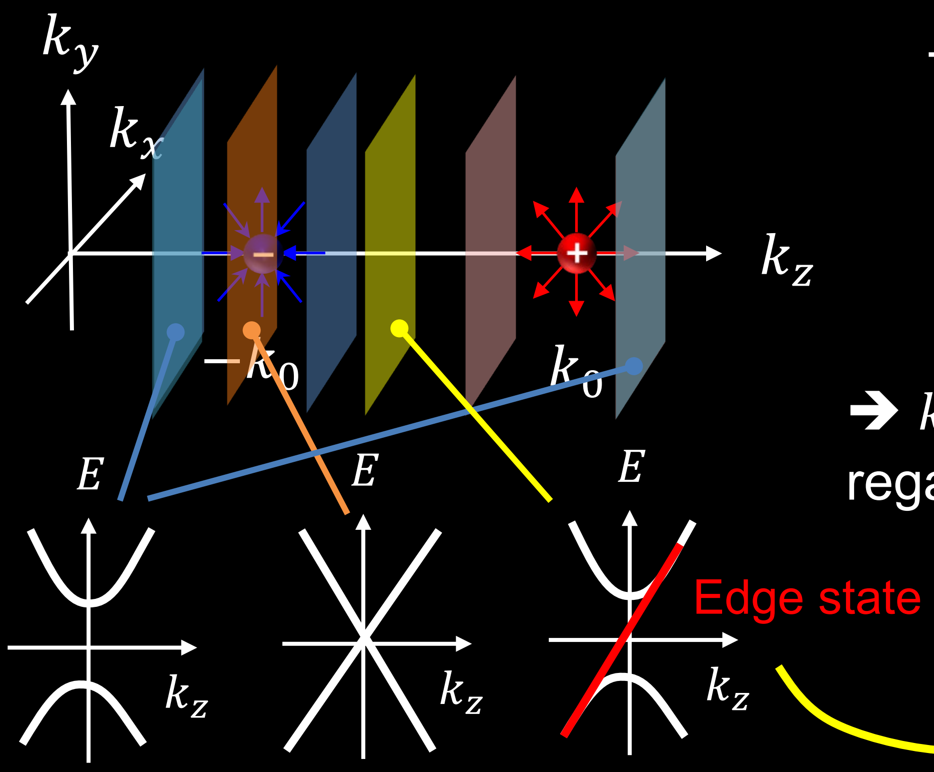

Insulator

Weyl
$(k = \pm k_0)$

Quantum Hall
$(-k_0 < k_z < k_0)$

To satisfy the Gauss's theorem,

$$C = \begin{cases} 1 & (-k_0 < k_z < k_0) \\ 0 & (k_z < -k_0, k_0 < k_z) \end{cases}$$

➔ k_x- k_y plane at $-k_0 < k_z < k_0$ can be regarded as the quantum Hall system.

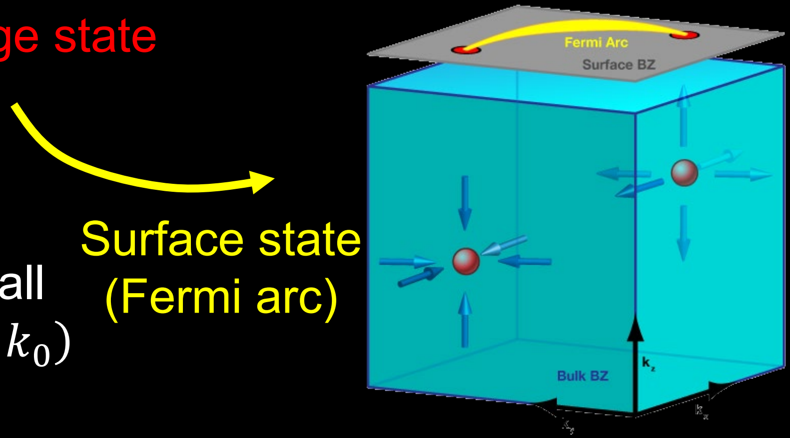

□ Hall conductivity

$$\sigma_{xy} = -\frac{e^2}{(2\pi)^2\hbar}\int_{-k_0}^{k_0} 1\, dk_z = -\frac{e^2}{(2\pi)^2\hbar}(2k_0)$$

Weyl semimetals with large fictitious field in the *k*-space

k-space

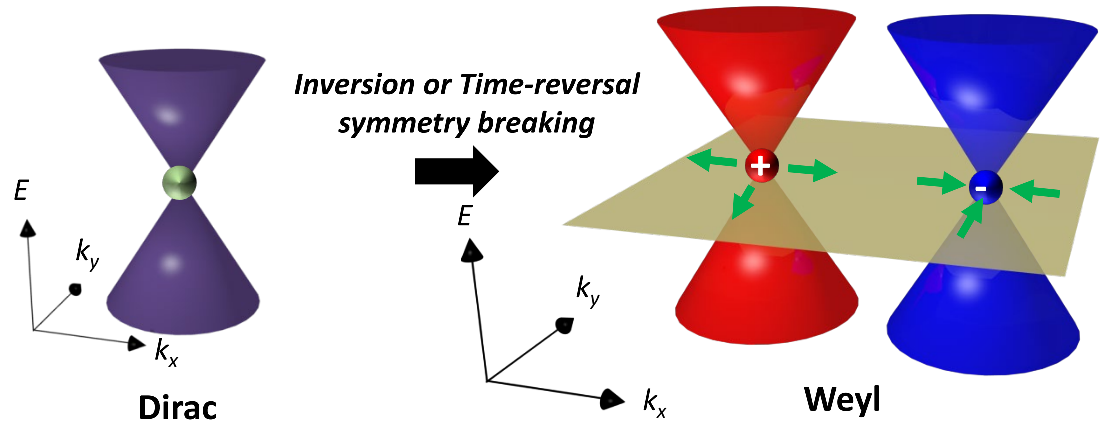

Berry curvature $\Omega(k)$

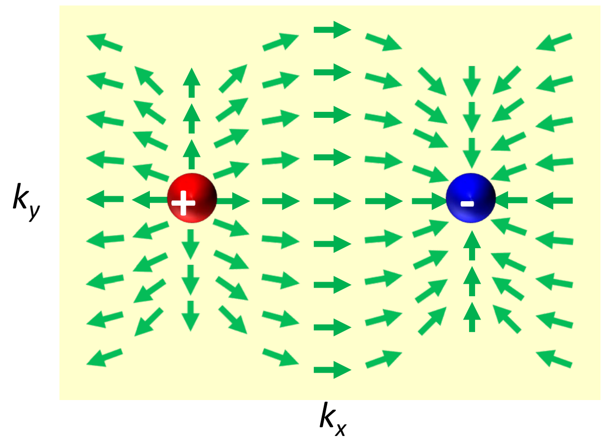

*Wan et al., PRB **83**, 205101 (2011), Armitage et al., RMP **90**, 015001 (2018).*

Real space

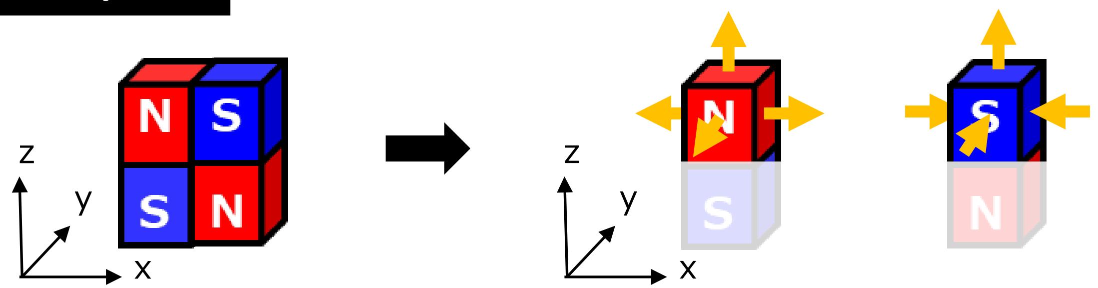

Magnetic field

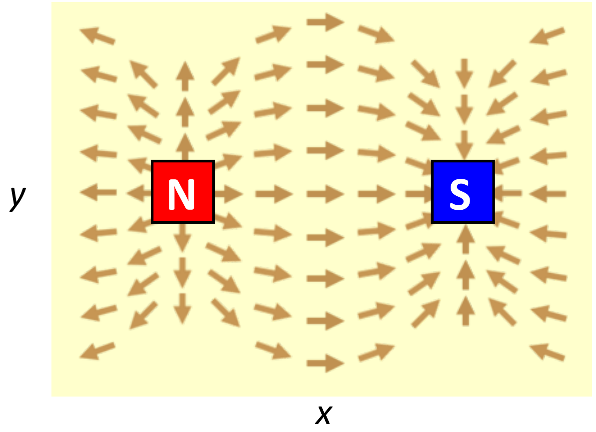

「Weyl magnets」

Magnetic structure allows to control the distribution of Weyl points

➡ **Large transverse response derived from $\Omega(k)$**

Weyl semimetals with large fictitious field in the *k*-space

k-space

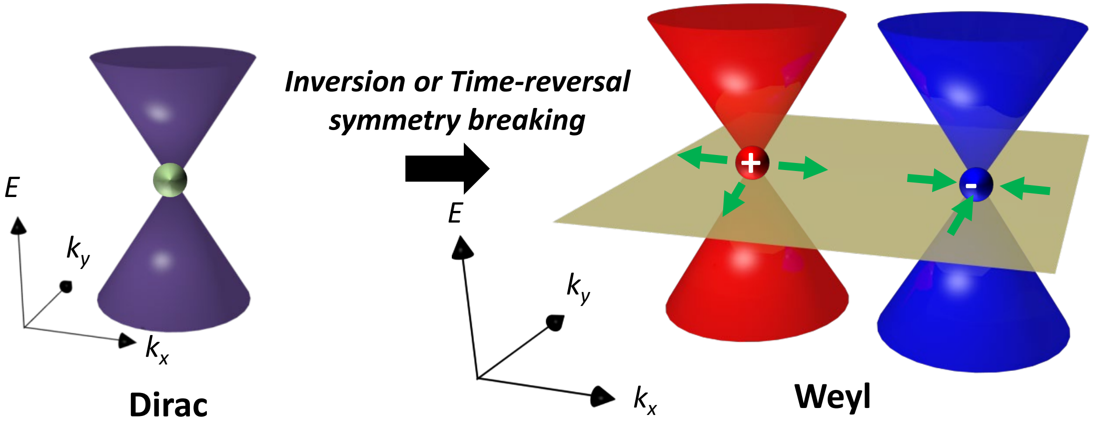

Wan et al., PRB **83**, 205101 (2011), Armitage et al., RMP **90**, 015001 (2018).

Berry curvature Ω(*k*)

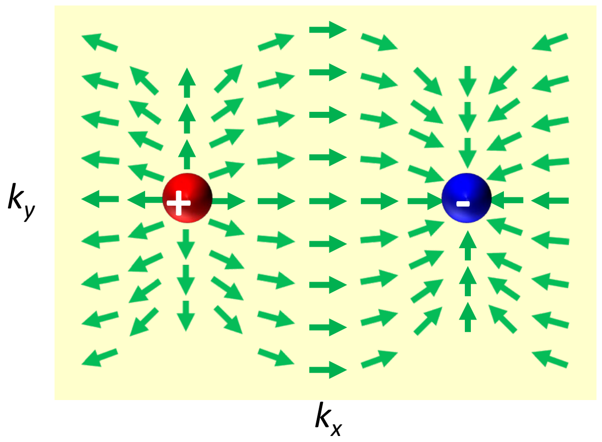

Topological magnets

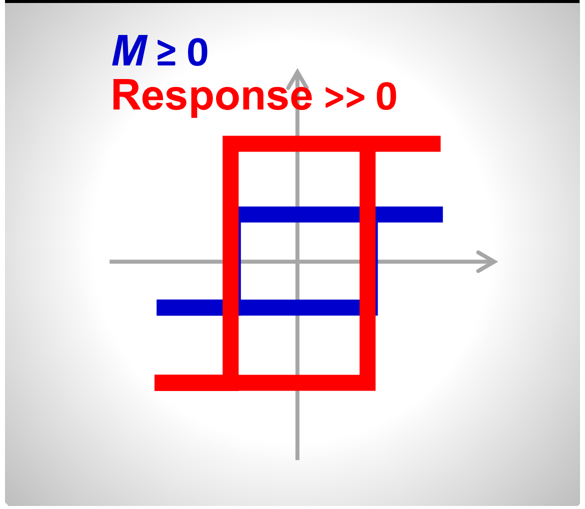

Ferromagnets (FMs)

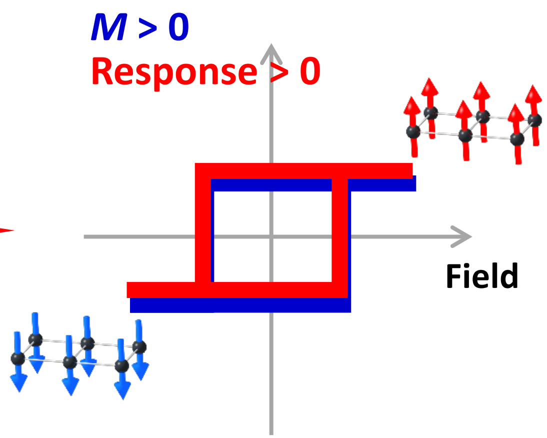

Antiferromagnets (AFMs)

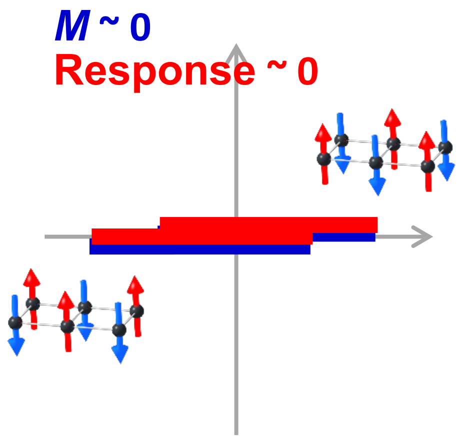

Weyl Magnets: Functional Magnets

Anomalous Hall Effect

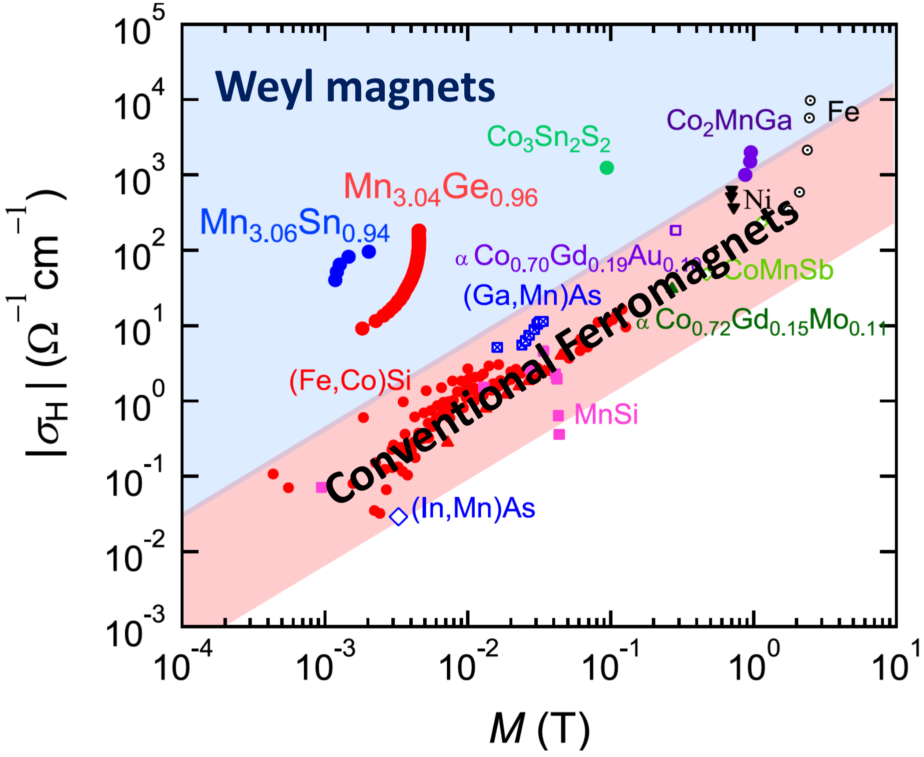

Anomalous Nernst Effect

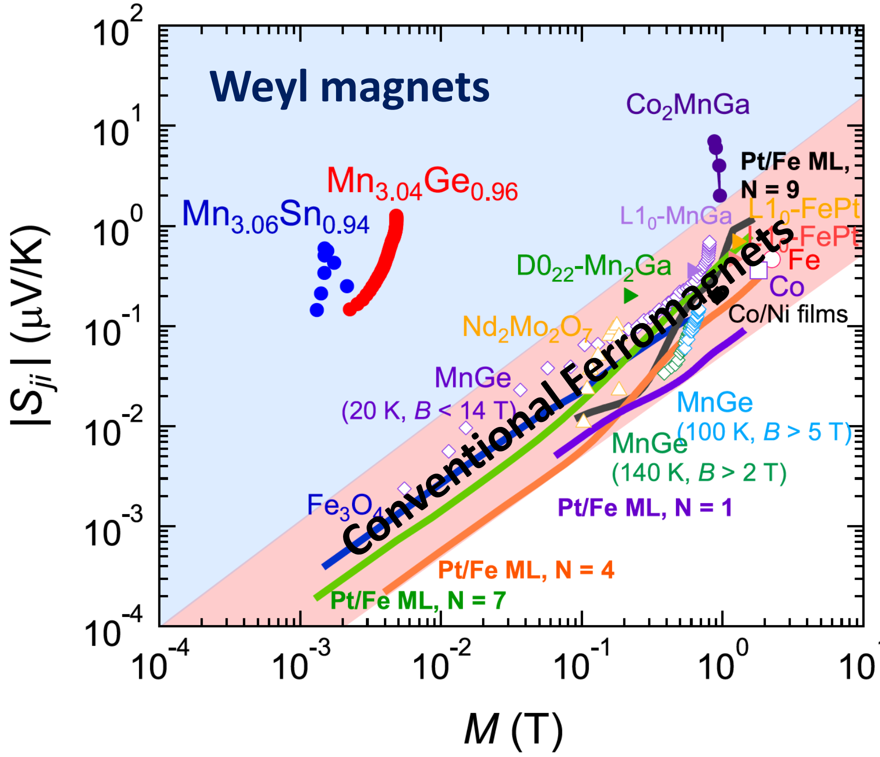

Non-volatile Memory

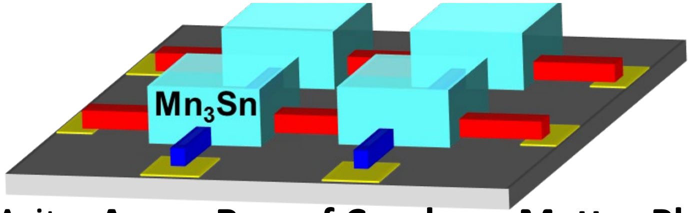

Thermoelectric Conversion

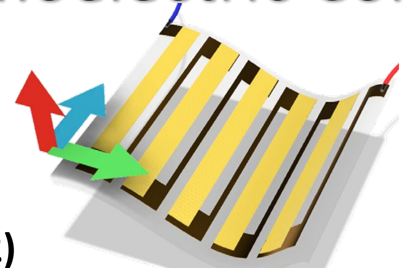

SN and R. Arita, **Annu. Rev. of Condens. Matter Phys., 13:119–42 (2022)**

Large responses are obtained irrespective of size of *M*.

Enhancement of ANE using topological band structures

Ikhlas⁺, Tomita⁺ et al., Nat. Phys. ***13****, 1085 (2017).*

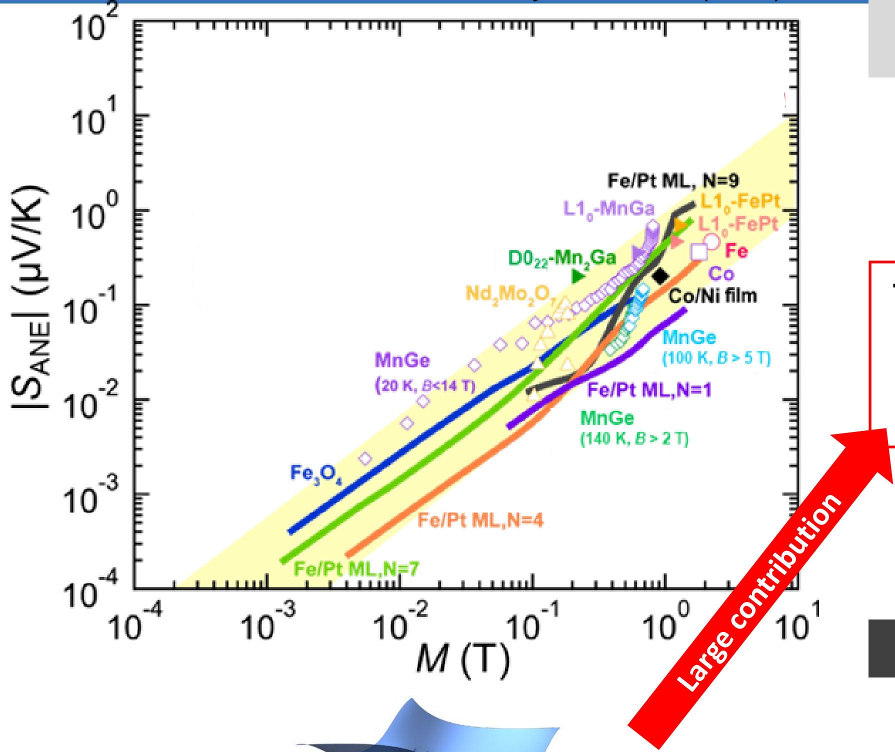

$$S_{\mathrm{ANE}} = \rho\left(-S_{\mathrm{SE}}\sigma_{yx} + \alpha_{yx}\right)$$

Hall conductivity

$$\sigma_{\mathrm{yx}}^{\mathrm{int}} = \epsilon_{xyz}\left(\frac{e^2}{\hbar}\right)\int_{\boldsymbol{k}}(2\pi)^{-3}\sum_n \Omega_{n,z}(\boldsymbol{k}) f\left(\varepsilon_{n,\boldsymbol{k}}\right)\mathrm{d}\boldsymbol{k}$$

Transverse TE conductivity

$$\alpha_{\mathrm{yx}} = \frac{k_{\mathrm{B}}}{e}\int_{\varepsilon}\epsilon_{xyz}\sum_{n,\boldsymbol{k}}\left\{\Omega_{n,z}(k)\delta\left(\varepsilon-\varepsilon_{n,\boldsymbol{k}}\right)\right\}s(\varepsilon,T)\mathrm{d}\varepsilon$$

Berry curvature

$$\boldsymbol{\Omega}_{n,z}(\boldsymbol{k}) = -2\mathrm{Im}\sum_{m\neq n}\frac{v_{nm,x}(\boldsymbol{k})v_{mn,y}(\boldsymbol{k})}{\{\varepsilon_m(\boldsymbol{k})-\varepsilon_n(\boldsymbol{k})\}^2}$$

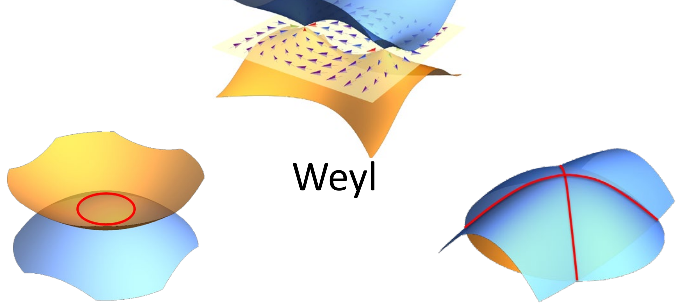

Weyl AFMs

Mn_3Sn: *Ikhlas, Tomita et al., Nature Phys.* ***13****, 1085 (2017).*
Mn_3Ge: *Chen et al., Nature Commun.* ***12****, 572 (2021).*
$YbMnBi_2$: *Pan et al., Nature Mater.* ***21****, 203 (2022).*

Weyl FMs

Co_2MnGa: *Sakai et al., Nature Phys.* ***14****, 1119 (2018).*
$Co_3Sn_2S_2$: *Guin et al., Adv. Mater.* ***31****, 1806622 (2019).*
$UCo_{0.8}Ru_{0.2}Al$: *Asaba et al., Sci. Adv.* ***7****, eabf1467 (2021).*

Nodal-web/-plane FMs

D0₃-Fe_3X (X = Al, Ga): *Sakai†,..,TH† et al., Nature* ***581****, 53 (2020).*
Fe_3Sn: *Chen et al., Sci. Adv.* ***8****, eabk1480 (2022).*

~10 times larger S_{ANE} than that of conventional FMs

Enhancement of ANE using topological band structures

Ikhlas⁺, Tomita⁺ et al., Nat. Phys. **13**, *1085 (2017).*

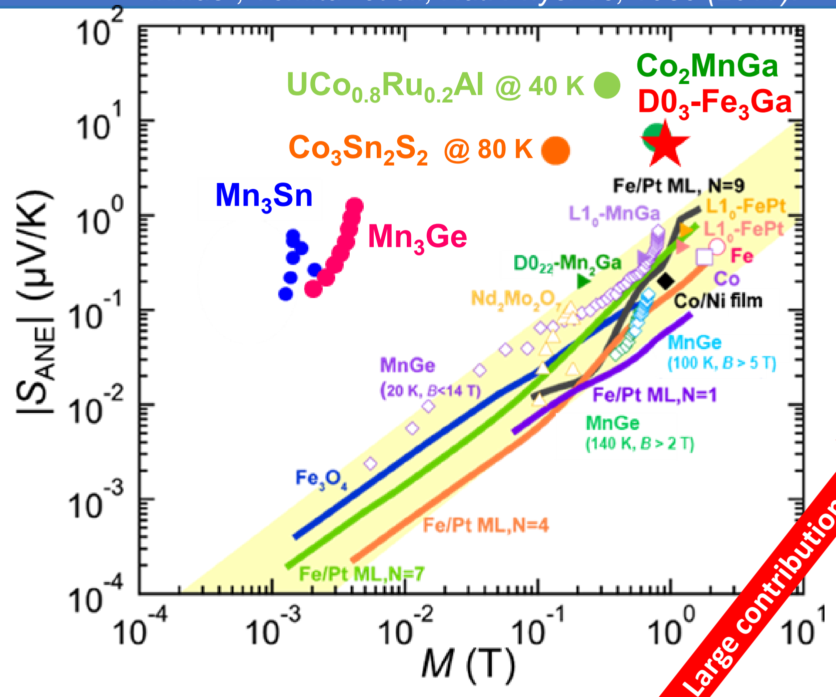

Large contribution

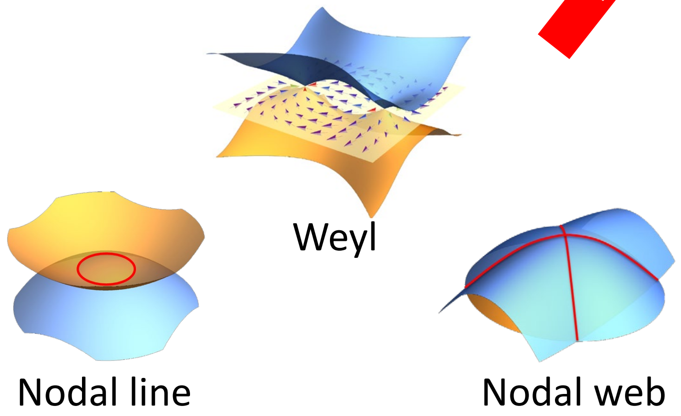

$$S_{\mathrm{ANE}} = \rho\left(-S_{\mathrm{SE}}\sigma_{yx} + \alpha_{yx}\right)$$

Hall conductivity

$$\sigma_{\mathrm{yx}}^{\mathrm{int}} = \epsilon_{xyz}\left(\frac{e^2}{\hbar}\right)\int_{\boldsymbol{k}}(2\pi)^{-3}\sum_{n}\Omega_{n,z}(\boldsymbol{k})f\left(\varepsilon_{n,\boldsymbol{k}}\right)\mathrm{d}\boldsymbol{k}$$

Transverse TE conductivity

$$\alpha_{\mathrm{yx}} = \frac{k_{\mathrm{B}}}{e}\int_{\varepsilon}\epsilon_{xyz}\sum_{n,\boldsymbol{k}}\left\{\Omega_{n,z}(\boldsymbol{k})\delta\left(\varepsilon-\varepsilon_{n,\boldsymbol{k}}\right)\right\}s(\varepsilon,T)\mathrm{d}\varepsilon$$

Berry curvature

$$\Omega_{n,z}(\boldsymbol{k}) = -2\mathrm{Im}\sum_{m\neq n}\frac{v_{nm,x}(\boldsymbol{k})v_{mn,y}(\boldsymbol{k})}{\{\varepsilon_m(\boldsymbol{k})-\varepsilon_n(\boldsymbol{k})\}^2}$$

Weyl AFMs

Mn_3Sn: *Ikhlas, Tomita et al., Nature Phys. 13, 1085 (2017).*

Mn_3Ge: *Chen et al., Nature Commun.* **12**, *572 (2021).*

$YbMnBi_2$: *Pan et al., Nature Mater.* **21**, *203 (2022).*

Weyl FMs

Co_2MnGa: *Sakai et al., Nature Phys. 14, 1119 (2018).*

$Co_3Sn_2S_2$: *Guin et al., Adv. Mater.* **31**, *1806622 (2019).*

$UCo_{0.8}Ru_{0.2}Al$: *Asaba et al., Sci. Adv.* **7**, *eabf1467 (2021).*

Nodal-web/-plane FMs

$D0_3$-Fe_3X (X = Al, Ga): Sakai†, et al., Nature 581, 53 (2020).

Fe_3Sn: *Chen et al., Sci. Adv.* **8**, *eabk1480 (2022).*

~10-100 times larger S_{ANE} than that of conventional FMs

Topological (Weyl) AFM Mn_3Sn

Mn_3Sn : Chiral antiferromagnetic order (T_N ~ 430 K)

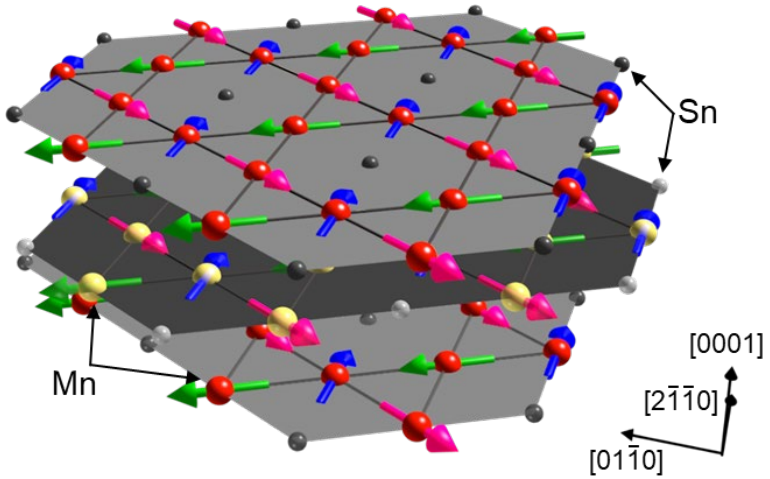

Anomalous Hall effect

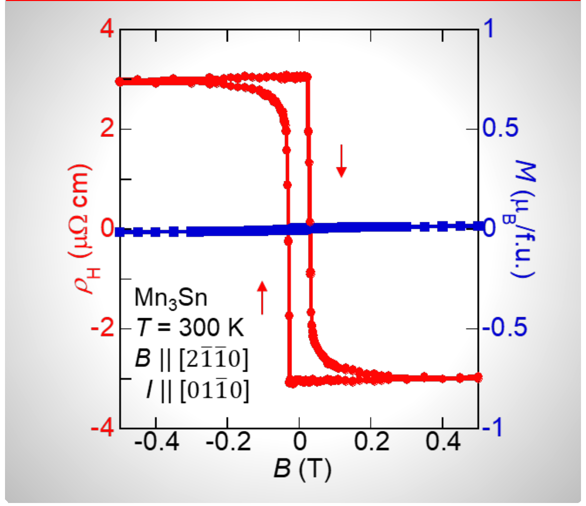

*SN, Kiyohara, & Higo, Nature **527**, 212 (2015).*

Order parameter：
Cluster magnetic octupole
*Suzuki et al., PRB **95**, 094406 (2017).*

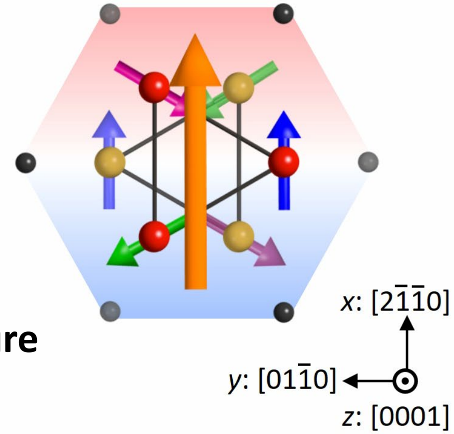

【Real space】
Magnetic structure

Berry curvature
Ω(*k*)

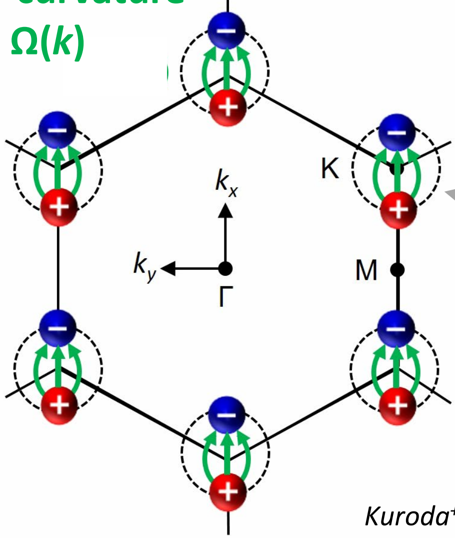

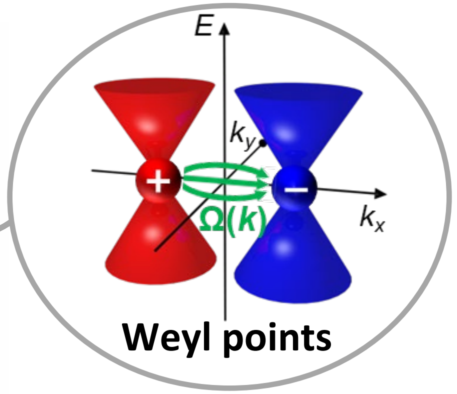

【Momentum space】
Electronic structure

*Kuroda⁺, Tomita⁺ et al., Nat. Mater. **16**, 1090 (2017).*

Antiferromagnets exhibiting large transverse responses

Large transverse responses of Weyl AFM Mn_3Sn

Magneto-optical Kerr effect

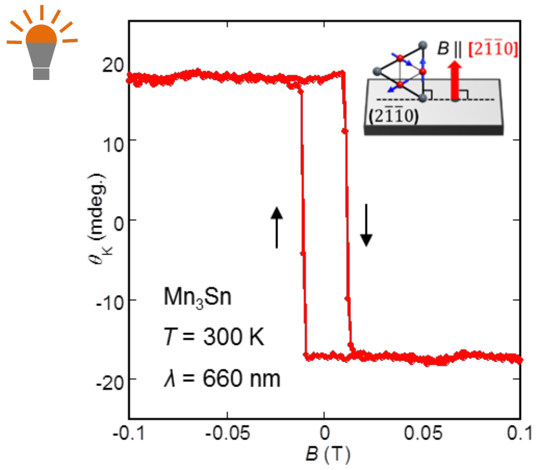

TH et al., Nat. Photon. **12**, 73 (2018).

Anomalous Nernst effect

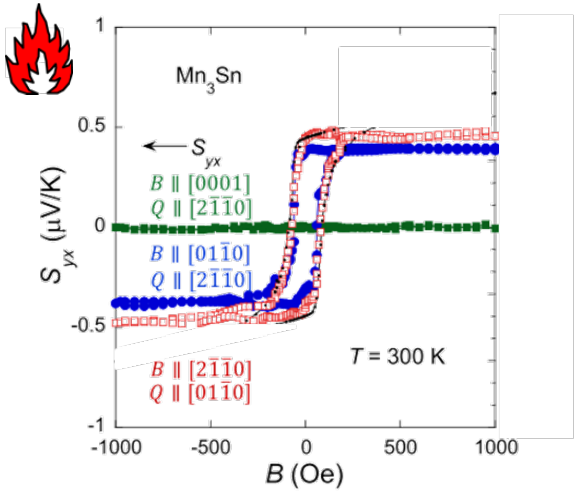

Ikhlas, Tomita et al., Nat. Phys. **13**, 1085 (2017).

Anomalous Hall effect

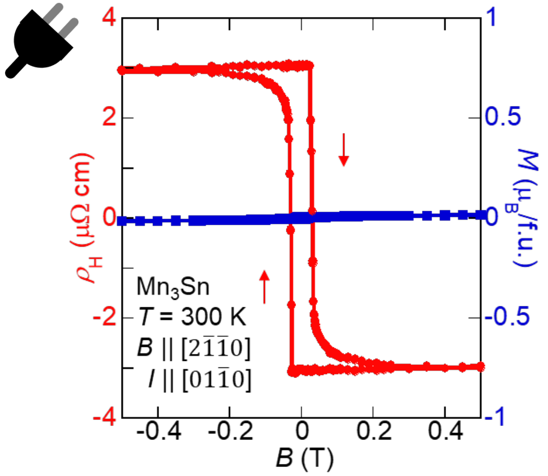

SN, Kiyohara, & Higo, Nature **527**, 212 (2015).

M independent ANE of Weyl AFM Mn_3Sn

Anomalous Nernst effect

M. Ikhlas T. Tomita

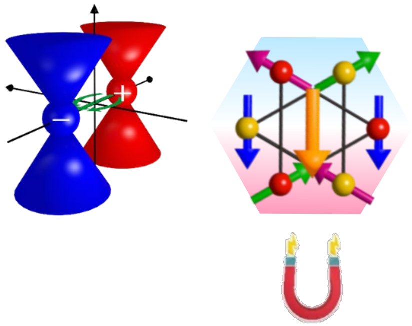

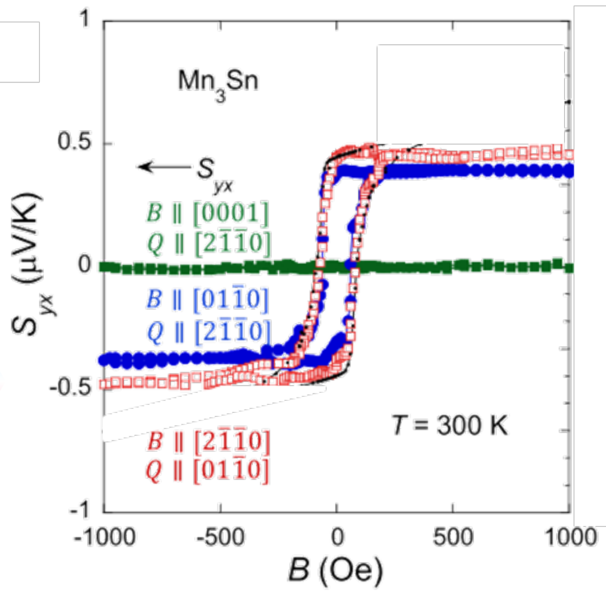

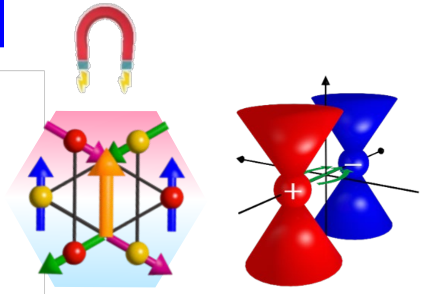

Ikhlas, Tomita et al., Nat. Phys. ***13****, 1085 (2017).*

■ Large spontaneous ANE at room temperature

M independent ANE ∝ Ω(k) ~ 100 T

$$S_{(A)NE} = \underbrace{Q_0 B + Q_S \mu_0 M}_{\sim 0.002\ \mu V/K} + \boxed{S_{ANE}^{AF} \sim -0.4\ \mu V/K} \fallingdotseq \text{FM metals}$$

(0 T → B; 0.005 μ_B → M)

$$S_{ANE} = \rho\left(\alpha_{yx} - S_{SE}\sigma_{yx}\right) \blacktriangleright \rho\alpha_{yx} \sim -0.5\ \mu V/K > \rho S_{SE}\sigma_{zx} \sim -0.1\ \mu V/K$$

$\rho\alpha_{yx}$: ∝ Ω(k) around E_F; $\rho S_{SE}\sigma_{zx}$: ∝ Ω(k) below E_F

ANE induced by large Ω(k) from topological band structures

Topological (Weyl) ferromagnet Co_2MnGa

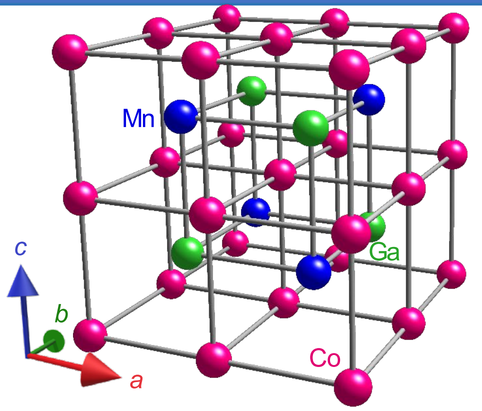

$L2_1$-ordered Co_2MnGa

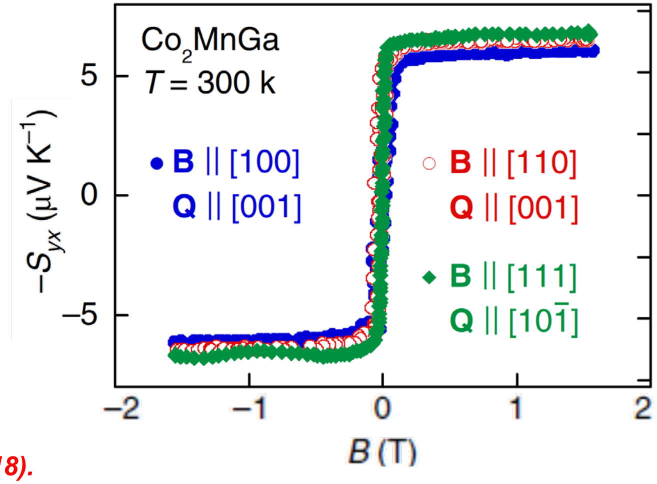

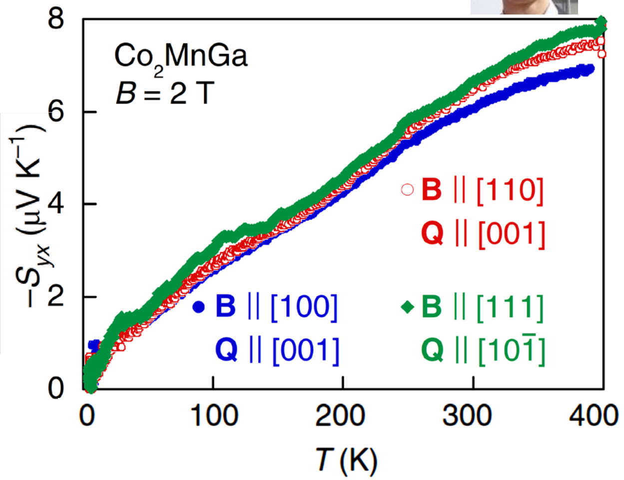

[Bulk] ***Sakai et al., Nature Phys. 14, 1119 (2018).***
Belopolski et al., Science 365 1278 (2019).

[Film] *Reichlova et al., APL **113**, 212405 (2018).*
*Sumida et al., Commun. Mater. **1**, 89 (2020).*
*Budai,.., TH et al., APL **122**, 102401 (2023).*

$$S_{yx} = \rho_{xx}(\alpha_{yx} - S_{yy}\sigma_{yx})$$

around E_F below E_F

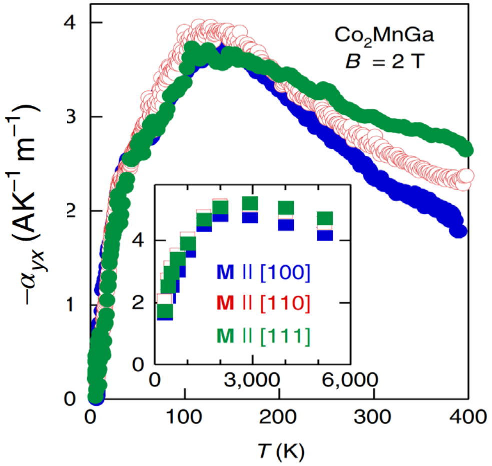

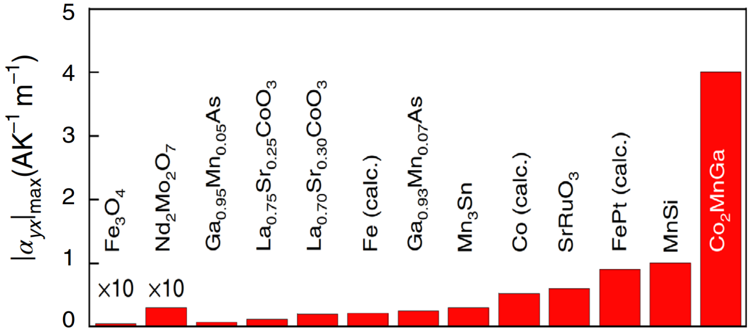

Largest ANE @ $T \geqq$ RT (6 μV/K @ RT, 8 μV/K @ 400 K)

Topological band structure of Co_2MnGa

Weyl points

Lifshitz transition

Sakai et al., Nature Phys. ***14****, 1119 (2018).*

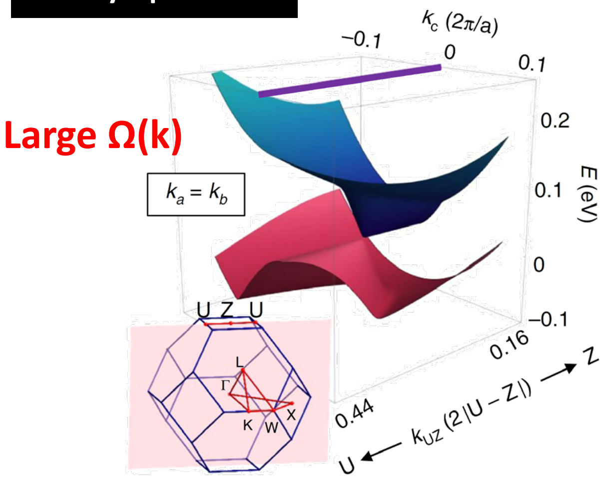

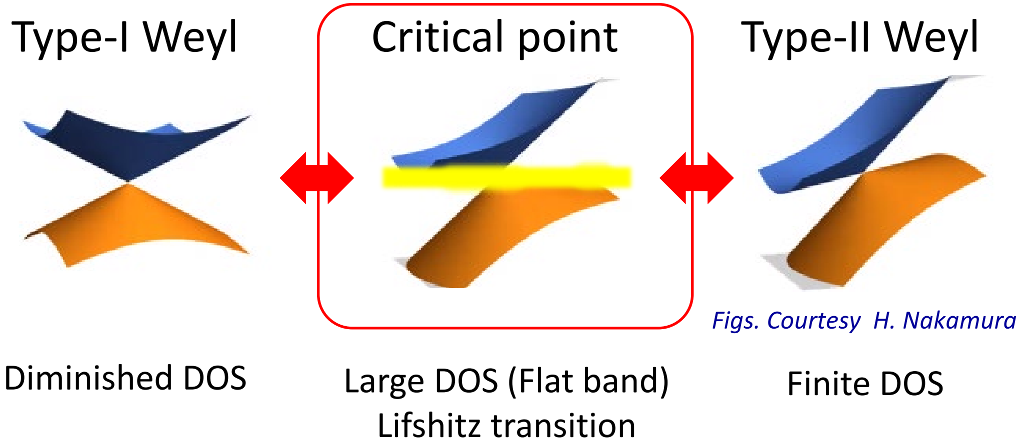

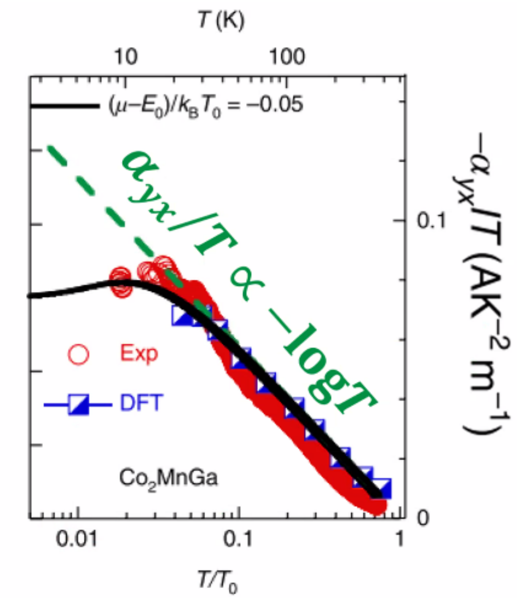

< 20K

$$\alpha_{yx} \approx -\frac{\pi^2}{3}\frac{k_B{}^2 T}{|e|}\frac{\partial \sigma_{yx}}{\partial E_F}$$

➡ α_{yx}/T = Constant (Mott relation)

≥ 20K

$$\alpha_{yx} \approx \alpha_{yx}{}^{max}\frac{T}{T_0}\log\left(\frac{|\mu - E_0|}{k_B T_0}\right)$$

➡ $\alpha_{yx}/T = -\log T$

$$k_B T_0 \approx C(k_0)\hbar v_1 k_0$$

$$\alpha_{yx}^{max}(k_0) = -\frac{k_B^2|e|T_0}{12\hbar^2 v_1 \exp(1)} \approx \frac{50}{a}\sin\left(\frac{k_0 a}{2}\right)\exp\left[-4\tan\left(\frac{k_0 a}{2}\right)\right]\mathrm{AK^{-1}m^{-1}}$$

suggests quantum Lifshitz transition

Large Ω(k) at Weyl points & DOS due to quantum Lifshitz transition

Nodal-web ferromagnet $D0_3$-Fe_3X (X = Ga, Al)

T. Koretsune

$D0_3$-Fe_3X (X = Ga, Al)

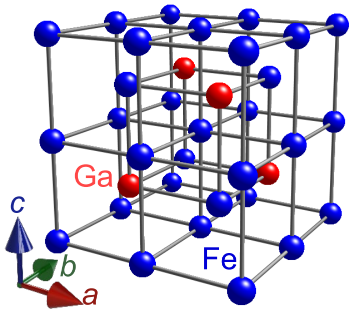

Calc. for ~1300 samples using MI

Formula	Space group	α_{max} ($A K^{-1} m^{-1}$)
Fe_3Pt	$Pm\bar{3}m$	6.2
Fe_3Ga	$Fm\bar{3}m$	3.0
Fe_3Al	$Fm\bar{3}m$	2.7

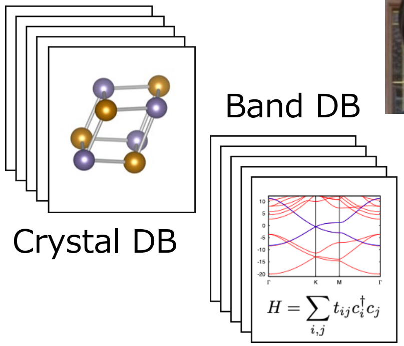

[Bulk & Film ($D0_3$)] *Sakai†,.., TH† et al., Nature* ***581****, 53 (2020).*

Minami et al., PRB ***102****, 205128 (2020).*

A. Sakai

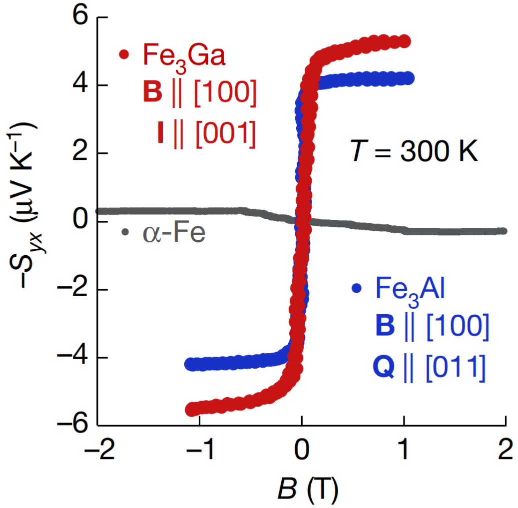

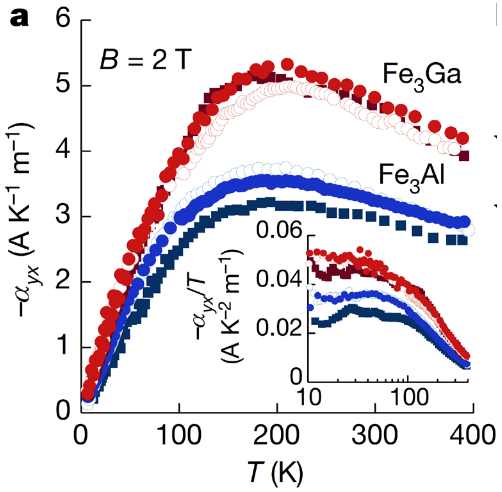

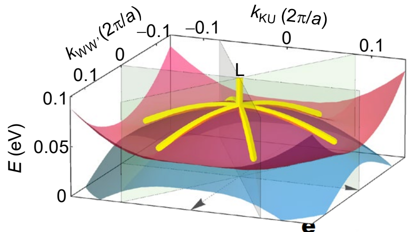

S. Minami

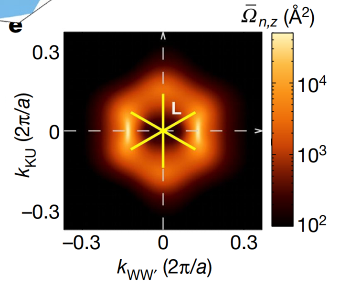

- **Giant ANE comparable to Co_2MnGa (S_{ANE} ~ 5.5 μV/K @ RT)**
- **Binary systems consisting of safe & inexpensive elements**

[Film (B2 ? A2?)] *Nakayama et al.,PRM* ***3****, 114412 (2019).*
Zhou, Sakuraba, APEX ***13****, 043001 (2020).*

Heat flux sensor

a wide variety of sensors 「Thermal sensors: 100 billion units by 2025」

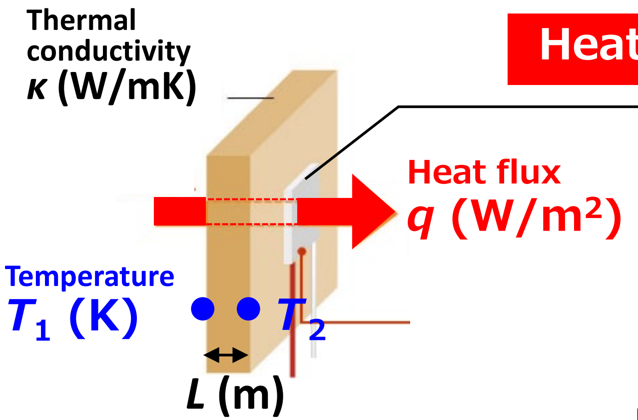

Heat Flux sensor

Denso HP

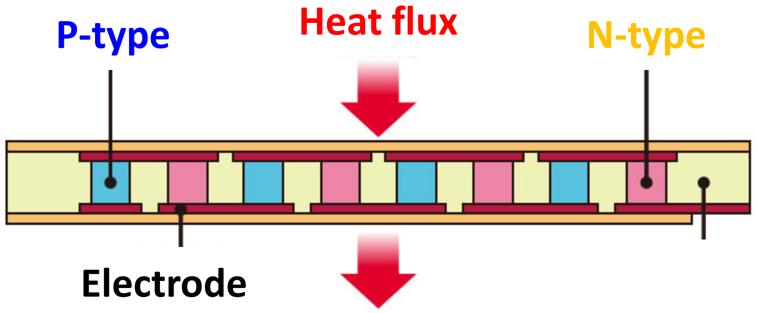

Heat flux $q = \kappa(T_1 - T_2)/L$

Sensitivity (1 × 1 cm^2)

10 μV/(W/m^2) (100 mV/W)

Visualizing the heat flow

- Heat dissipation/reception around an engine
- Abnormal heat generation in electronics
- Thermal conductivity (insulation)
- Health Care (deep body temperature))

ANE-type heat flux sensor

Anomalous Nernst effect

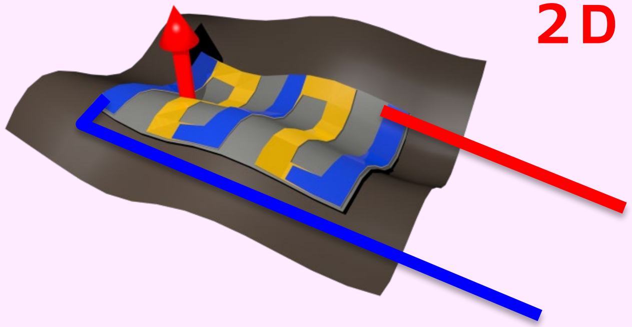

Flexible, Simple, Large area

Sensitivity

0.001 - 0.01 mV/W・m^{-2}

Mn_3Sn : **0.35** μV/K

Fe_3Ga : **~6** μV/K

Seebeck effect

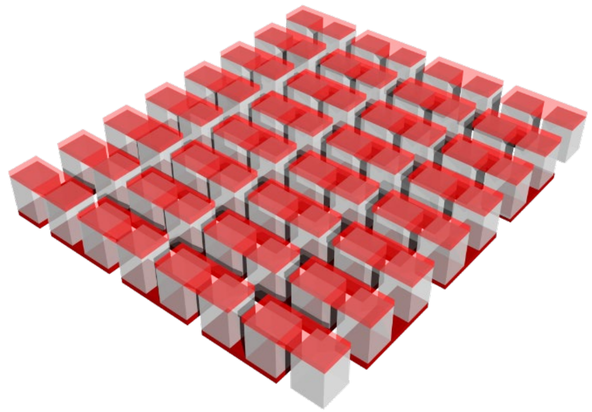

Sensitivity (1×1 cm²)

0.01 mV/W・m^{-2}

Denso HP

e.g., Zhou & Sakuraba, APEX ***13****, 043001 (2020); TH et al., Adv. Funct. Mater.* ***31****, 2008971 (2021)…*

Flexible heat flow sensor using thin-film fabrication

Price : SE $500 → ANE $1-10

ANE-type heat flux sensor

Anomalous Nernst effect

Heat Flux

2 D

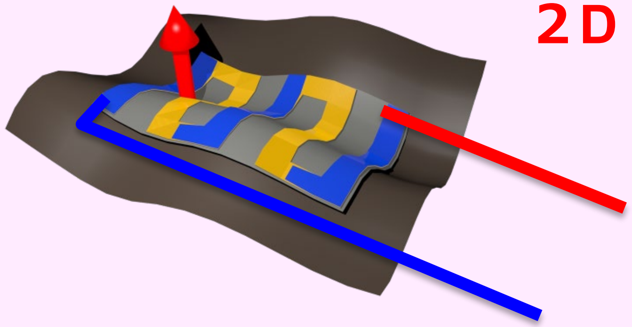

Flexible, Simple, Large area

Sensitivity

0.001 - 0.01 mV/W · m^{-2}

Mn_3Sn : **0.35** μV/K

Fe_3Ga : **~6** μV/K

Problem: Shape anisotropy

Undesired | **Ideal**

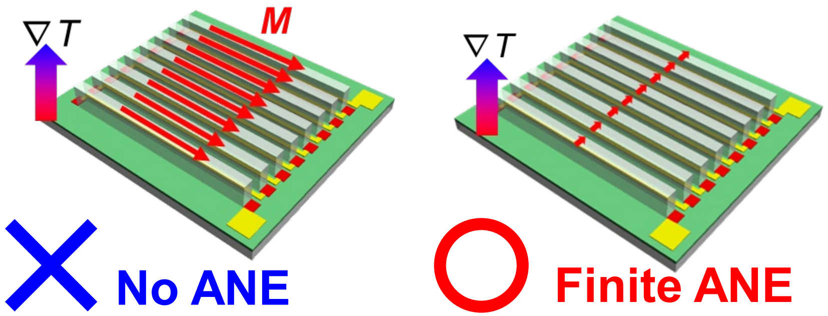

No ANE | **Finite ANE**

Magnetic hardness parameter κ

$\kappa = (K/\mu_0 M^2)^{1/2}$

Large κ ➡ ideal arrangement

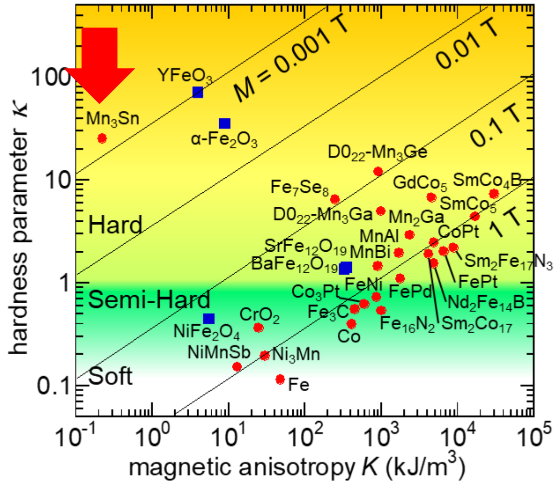

e.g., Zhou & Sakuraba, APEX ***13****, 043001 (2020); TH et al., Adv. Funct. Mater.* ***31****, 2008971 (2021)…*

Flexible heat flow sensor using thin-film fabrication

Price : SE \$500 → ANE \$1-10

Collaboration work with Nitto Denko Corp.

Nitto
Innovation for Customers

Tanaka, et al., Advanced Materials (2023).

Roll to Roll fabrication

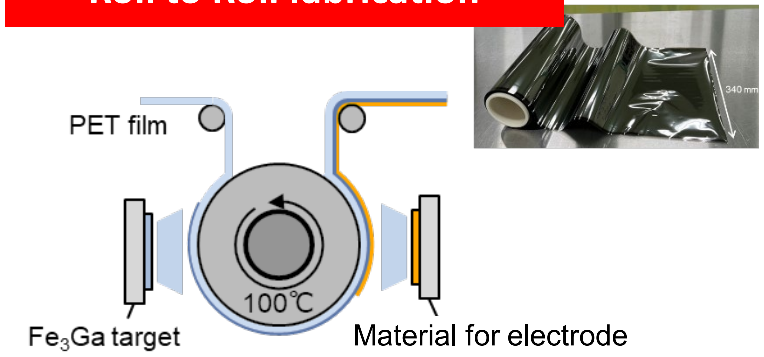

H. Tanaka Y. Nakanishi H. Machinaga

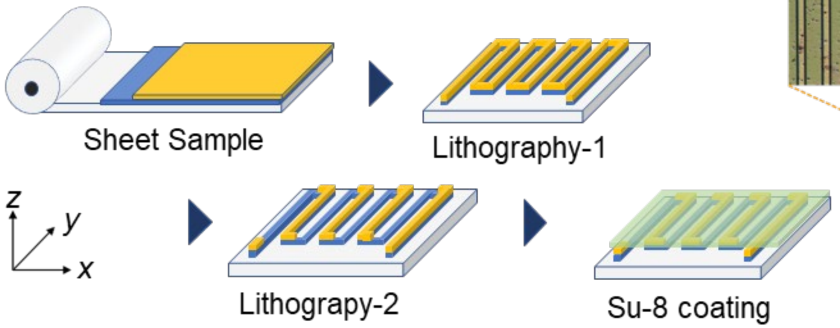

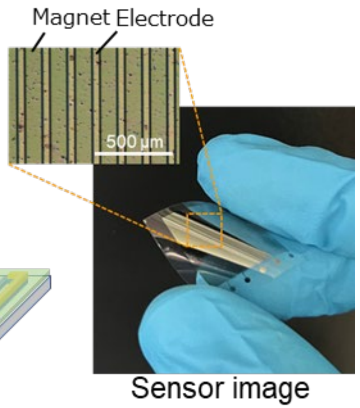

Direct sensing of perpendicular heat flux

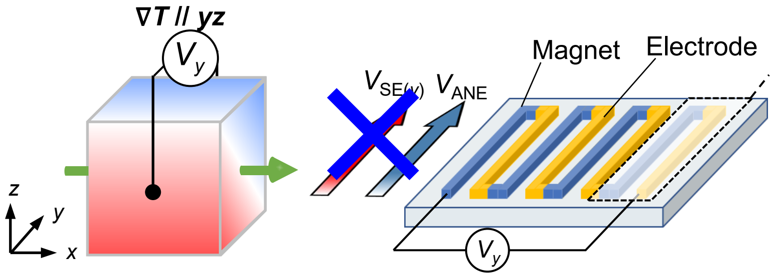

$S_{SE}^{Magnet} = S_{SE}^{Electrode}$

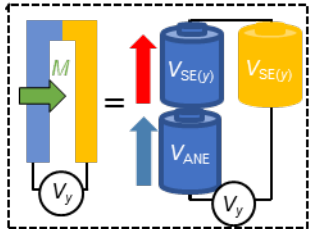

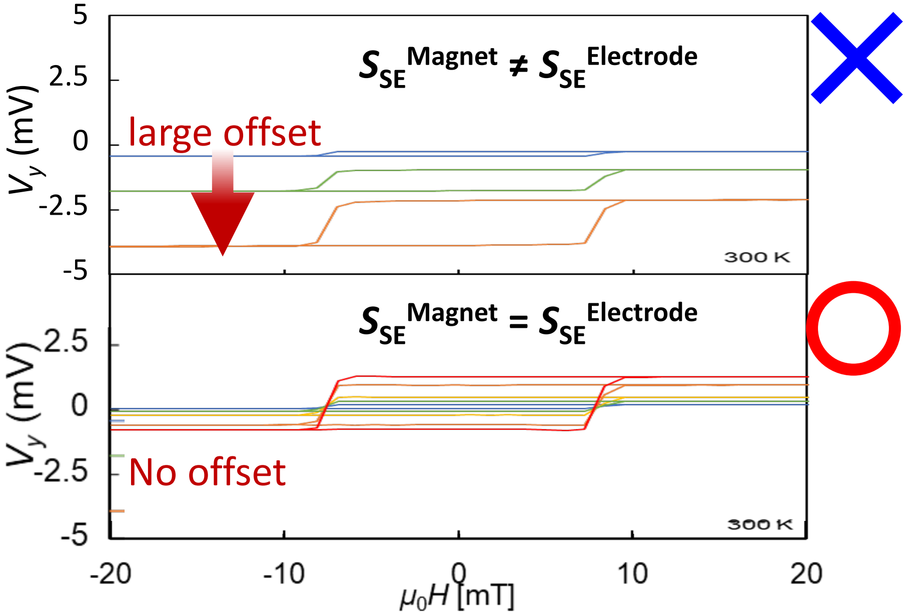

Mass producible flexible sensor for perpendicular heat flux sensing

Plan

- Multipole Physics on Correlated Electron Systems
- Topological States in Magnetic Systems
- Physics of Antiferromagnetic Weyl Semimetals
- Physics of Multipolar Kondo Lattice Systems

Multipolar phenomena in Ce^{3+}-based systems

La-doped CeB_6 : *B*-*T* phase diagram featuring dipolar, quadrupolar, and octupolar orders

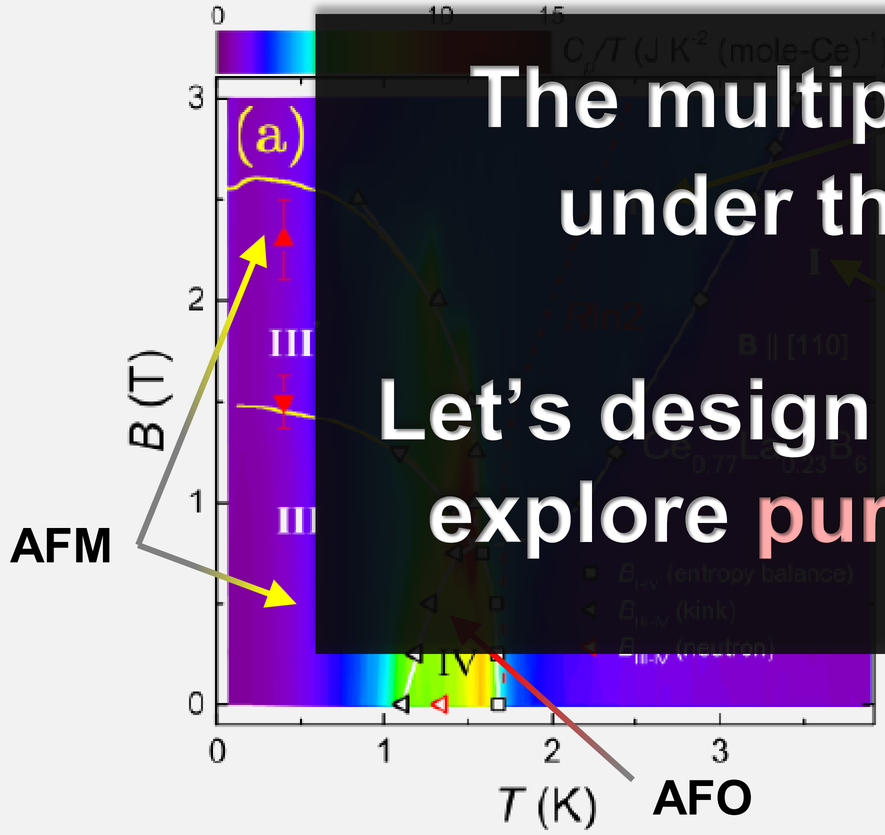

$Ce_3Pd_{20}Si_6$: Two electron localization transitions driven by dipolar and quadrupolar d.o.f

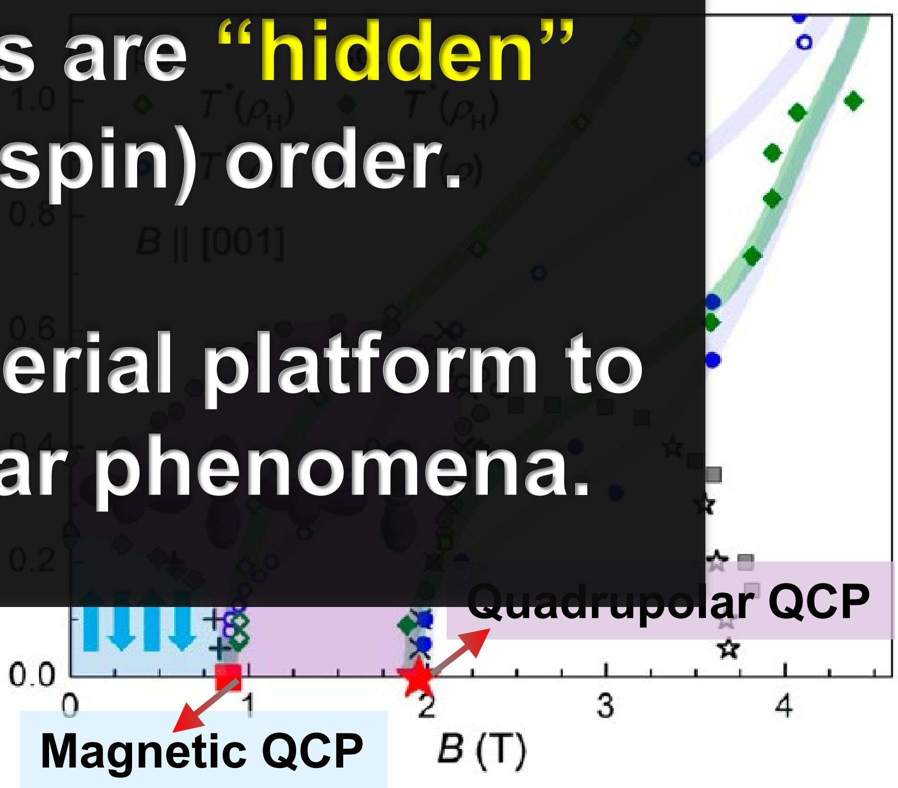

The multipolar orders are "hidden" under the dipolar (spin) order.

Let's design a new material platform to explore pure multipolar phenomena.

D. Jang et al., npj Quantum Mater (2017)

V. Martellia et al., PNAS (2019)

Cubic Pr^{3+} systems: Ideal platform for multipolar physics

4f Kramers doublet (e.g., Ce^{3+}, Yb^{3+})

- Odd number of f electrons
- Half-integer *J*
- Kramer’s theory: **double degeneracy protected by time-reversal symmetry**

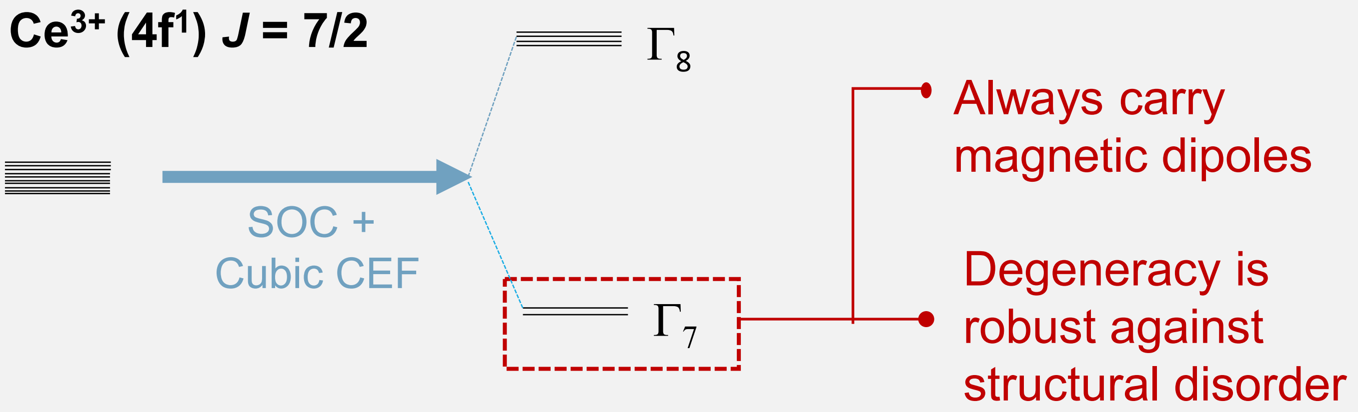

4f non-Kramers doublet (e.g., Pr^{3+})

- Even number of f electrons
- Integer *J*
- Double degeneracy is ***not*** protected by time-reversal symmetry but by **the local symmetry**

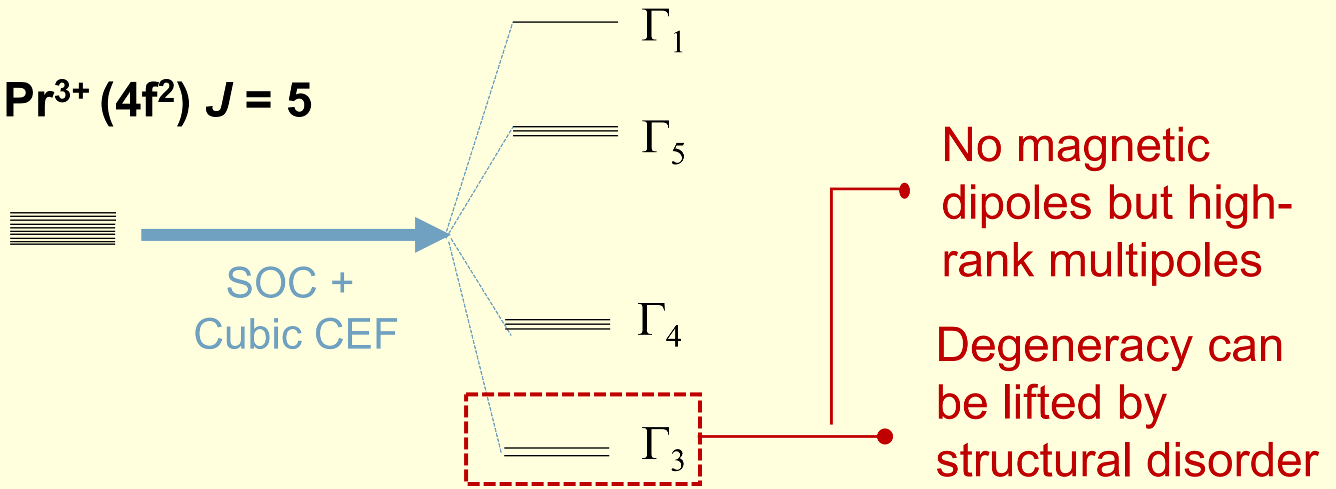

Cubic Pr^{3+} systems: Ideal platform for multipolar physics

$Pr(TM)_2Al_{20}$

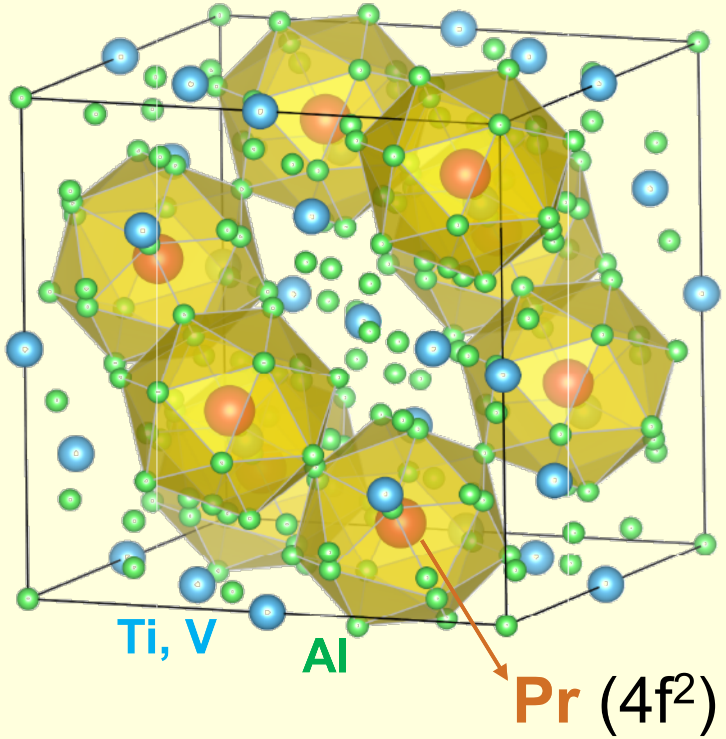

Frank-Kasper cages of 16 Al surrounding the Pr ion
→ strong *c-f* hybridization

CEF scheme of Pr^{3+} in local **cubic** environment

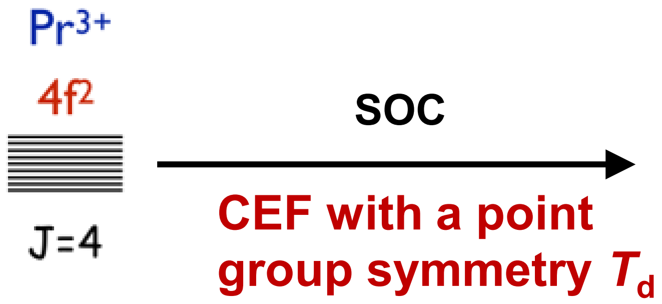

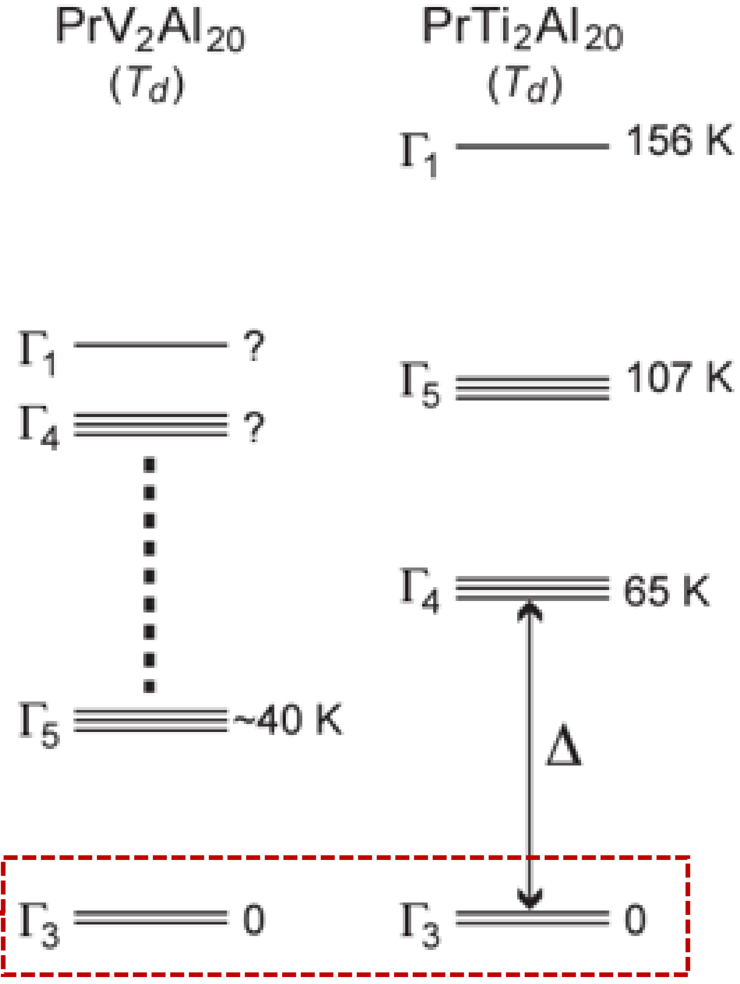

$$|\Gamma_3^+\rangle = \frac{1}{2}\sqrt{\frac{7}{6}}(|{+4}\rangle + |{-4}\rangle) - \frac{1}{2}\sqrt{\frac{5}{3}}|0\rangle$$

$$|\Gamma_3^-\rangle = \sqrt{\frac{1}{2}}(|{+2}\rangle + |{-2}\rangle)$$

Well-isolated non-Kramers doublet ground state

Cubic Pr^{3+} systems: Ideal platform for multipolar physics

Pr $(TM)_2Al_{20}$

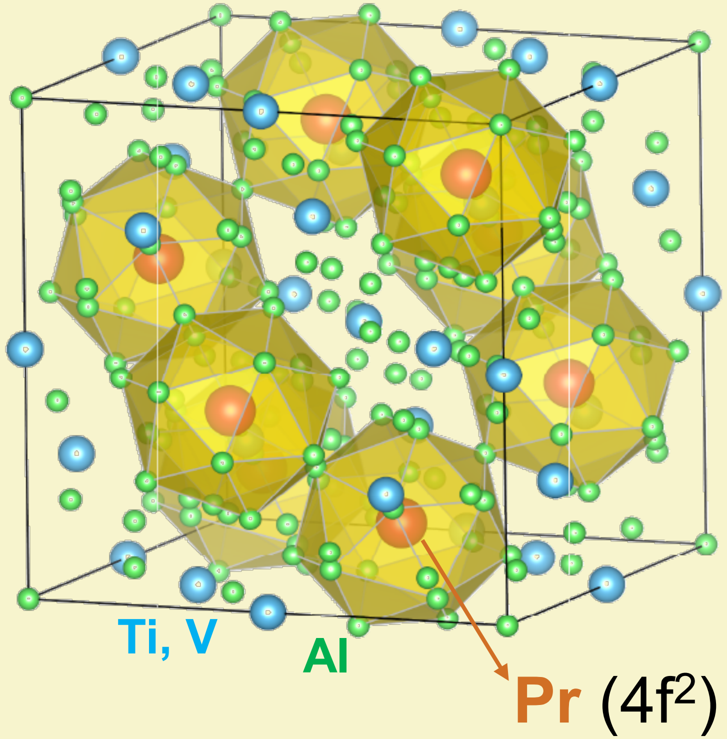

Frank-Kasper cages of 16 Al surrounding the Pr ion
→ strong *c-f* hybridization

CEF scheme of Pr^{3+}
in local **cubic**
environment

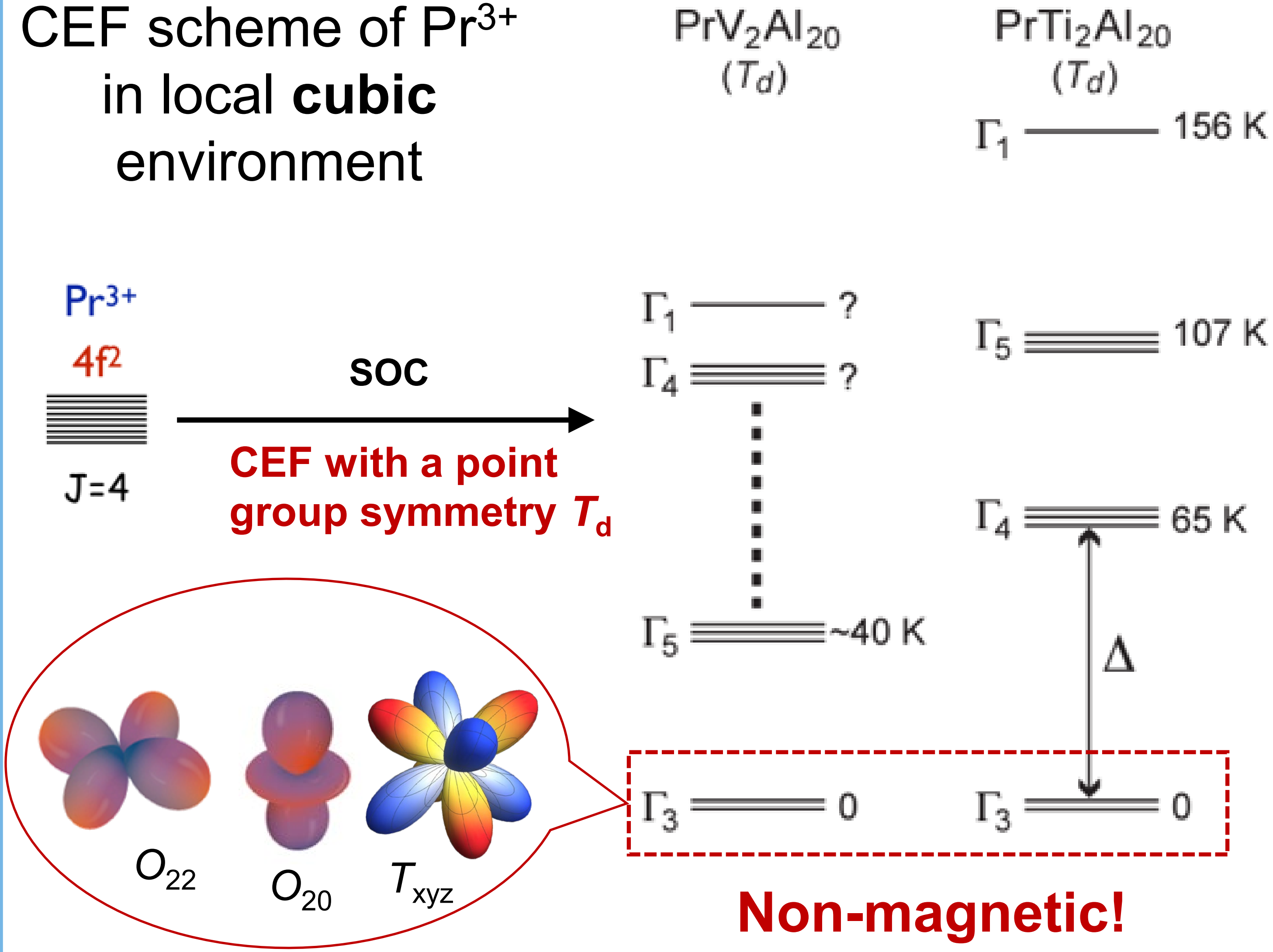

How do multipoles modify quantum phenomena?

Magnetic Kondo effect

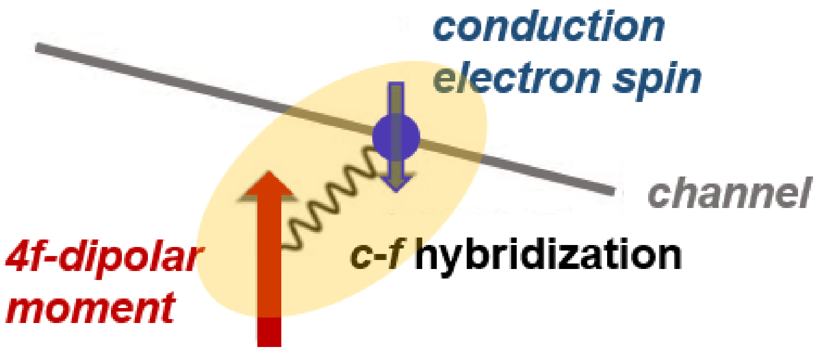

Single-channel Kondo model (k = 1) and **exact screening**

f electrons become itinerant and enter the Fermi surface in the **heavy-fermion Fermi liquid (FL) ground state**

$$\rho \sim AT^2 \qquad C/T \sim \frac{m^*}{m_0}\gamma_0$$

VS.

Quadrupolar Kondo effect

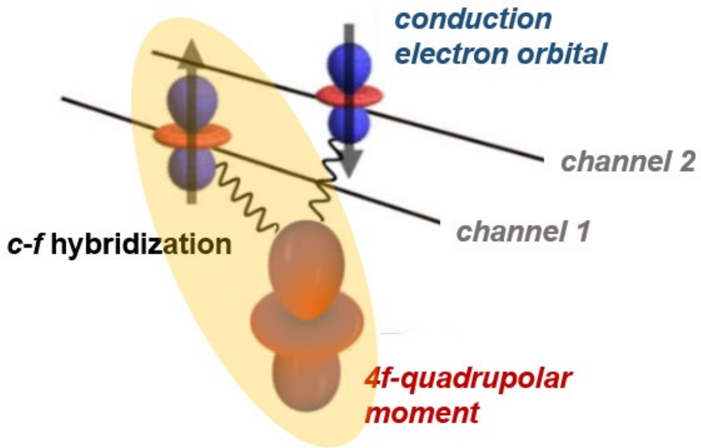

Two-channel Kondo model (k = 2) and **over-screening** D. L. Cox, Phys. Rev. Lett. (1987).

Residual entropy $S_0 = \frac{1}{2}R\ln 2$ **leads to a non-Fermi liquid (NFL) ground state**

$$\rho \sim T^{1/2},\ C/T \sim -\ln T,$$
$$\chi \sim T^{1/2} \text{ or } \sim -\ln T$$

How do multipoles modify quantum phenomena?

Magnetic Kondo effect

Single-channel Kondo model and **exact screening**

f electrons become itinerant and enter the Fermi surface in the **heavy-fermion Fermi liquid (FL) ground state**

$$\rho \sim AT^2 \qquad C/T \sim \frac{m^*}{m_0}\gamma_0$$

Quadrupolar Kondo effect

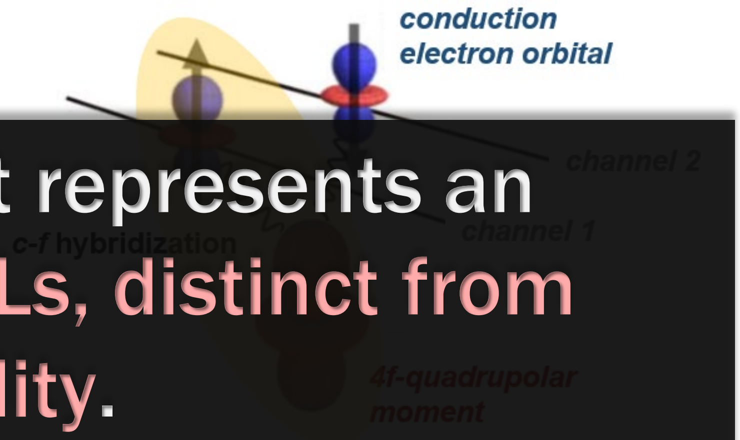

Two-channel Kondo model ($k = 2$) and **over-screening**

(1987).

Residual entropy $S_0 = \frac{1}{2} R \ln 2$ **leads** to a **non-Fermi liquid (NFL) ground state**

$$\rho \sim T^{1/2},\ C/T \sim -\ln T,$$

$\chi \sim T^{1/2}$ or $\sim -\ln T$

The multipolar Kondo effect represents an alternative route to novel NFLs, distinct from quantum criticality.

The NFL is intrinsic to the multipolar Kondo interaction and thus does not require fine-tuning of parameters.

Multipolar RKKY vs. Multipolar Kondo effect?

Modulated AFQ order in $PrPb_3$

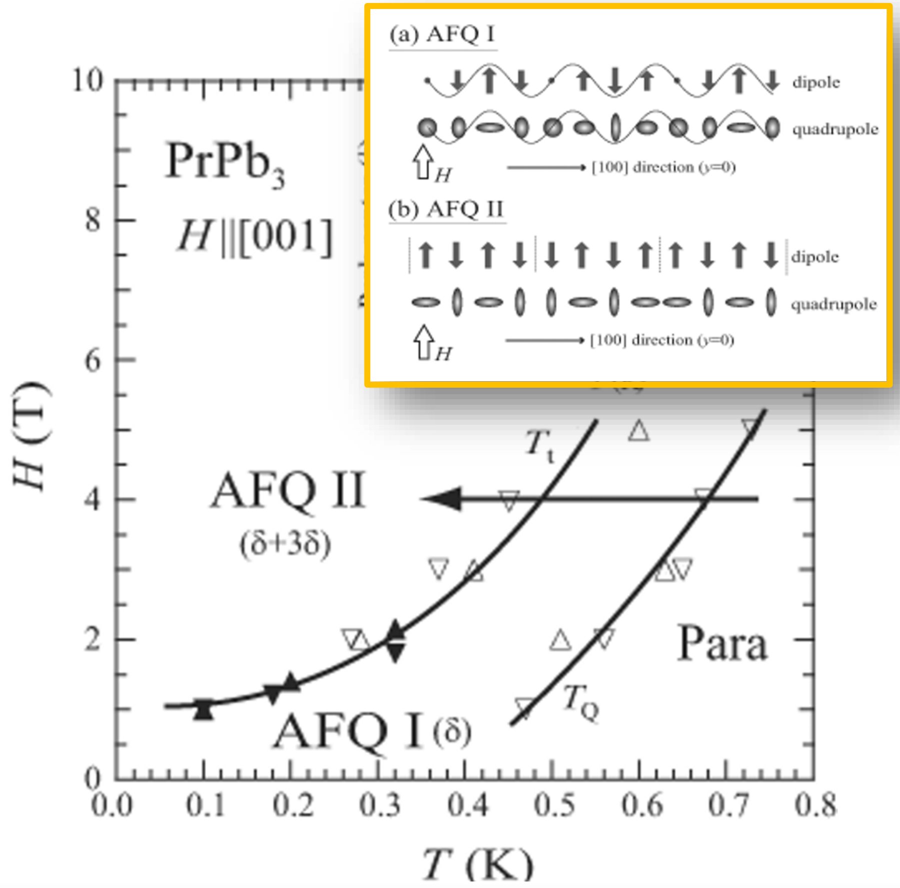

T. Ominaru *et al.*, PRL**94**, 197201 (2005)

Single-site multipolar Kondo effect in $Y_{1-x}Pr_xIr_2Zn_{20}$

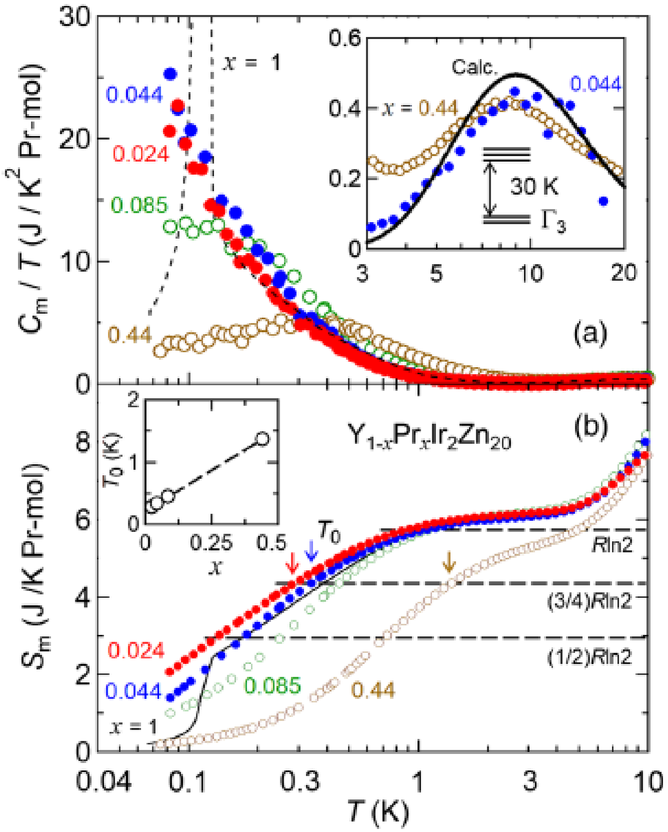

$PrIr_2Zn_{20}$ (x = 1)

AFQ order

Dilute

$Y_{1-x}Pr_xIr_2Zn_{20}$

Non-Fermi liquid

Y. Yamane *et al.*, PRL**121**, 077206 (2018)

Multipolar RKKY vs. Multipolar Kondo effect?

Modulated AFQ order in $PrPb_3$

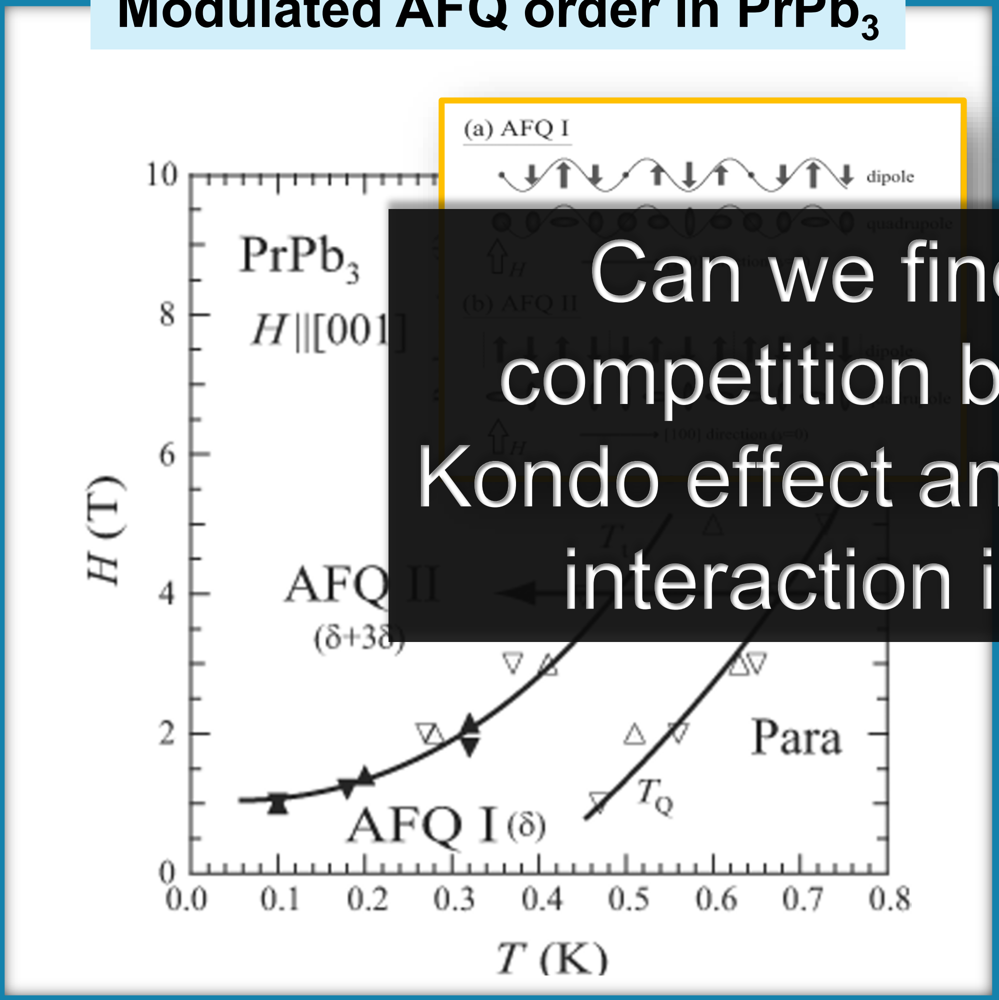

T. Ominaru *et al.*, PRL**94**, 197201 (2005)

Single-site multipolar Kondo effect in $Y_{1-x}Pr_xIr_2Zn_{20}$

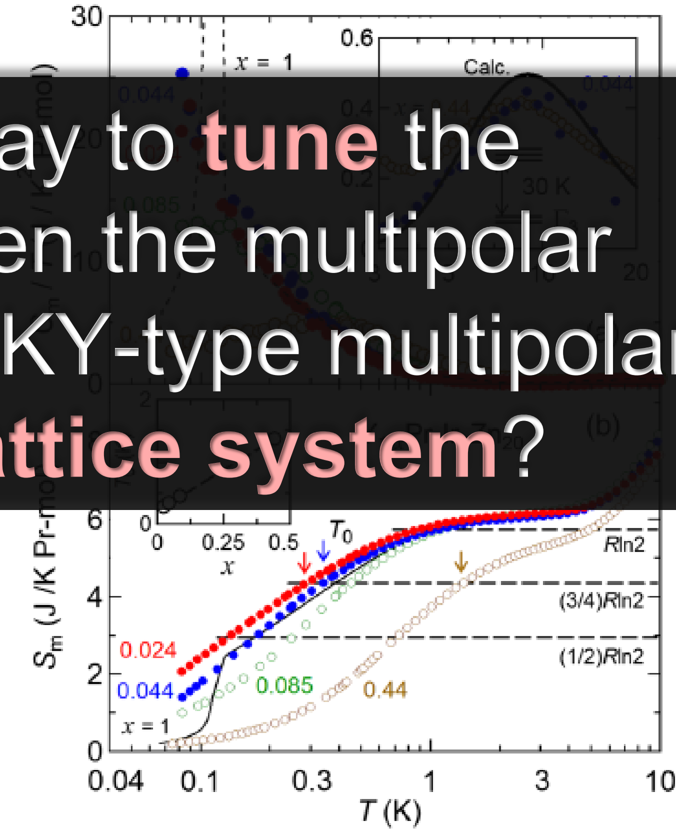

$PrIr_2Zn_{20}$ (x = 1)

AFQ order

Dilute

$Y_{1-x}Pr_xIr_2Zn_{20}$

Non-Fermi liquid

Y. Yamane *et al.*, PRL**121**, 077206 (2018)

Can we find a way to **tune** the competition between the multipolar Kondo effect and RKKY-type multipolar interaction in **a lattice system**?

Unifying themes of strongly correlated matters

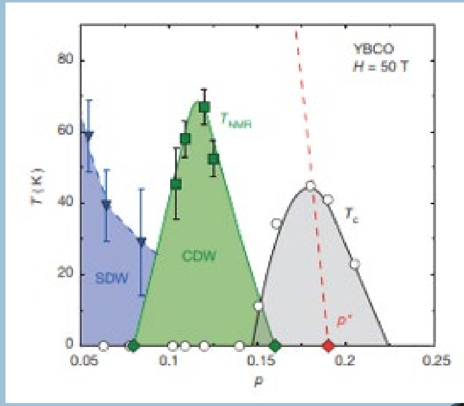

High-T_c cuprate

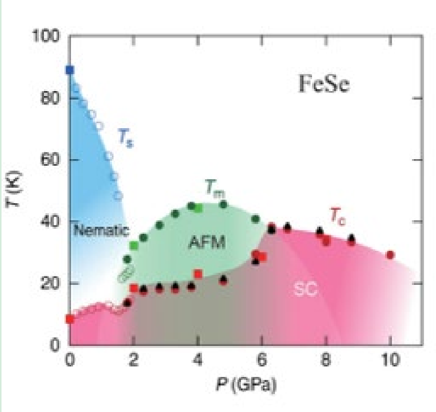

Fe-based SC

Universal properties among various material classes?

Organic SC

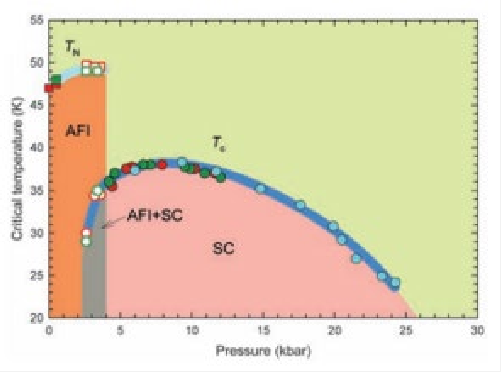

MATBG

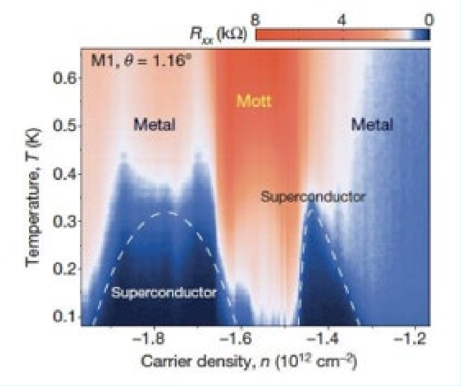

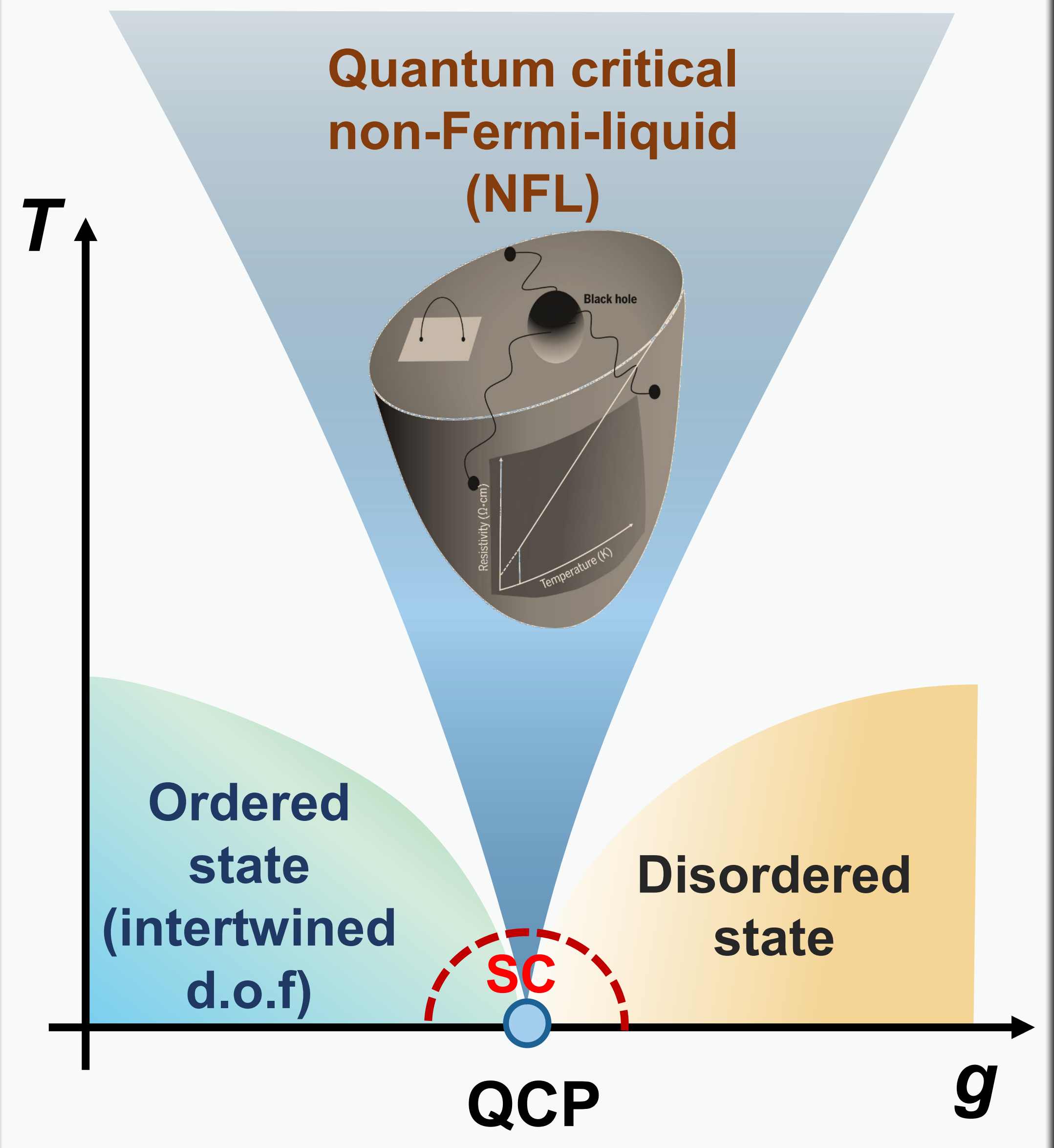

Unifying themes of strongly correlated matters

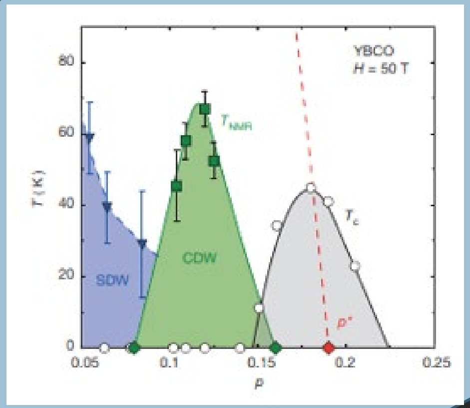

High-T_c cuprate

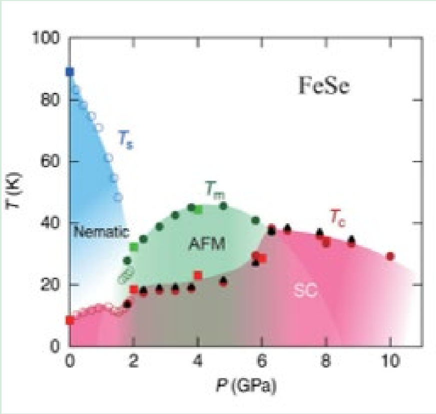

Fe-based SC

Universal properties among various material classes?

Organic SC

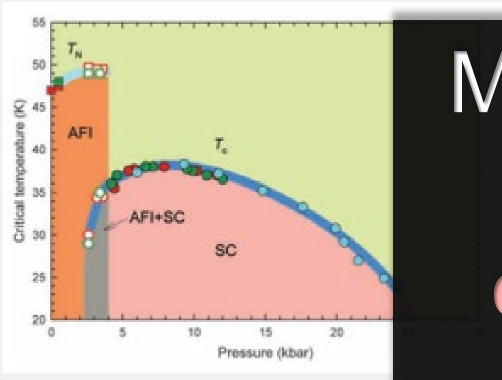

MATBG

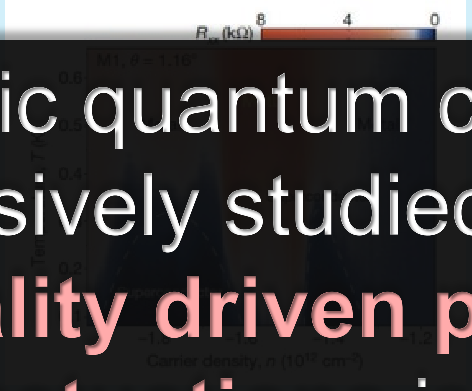

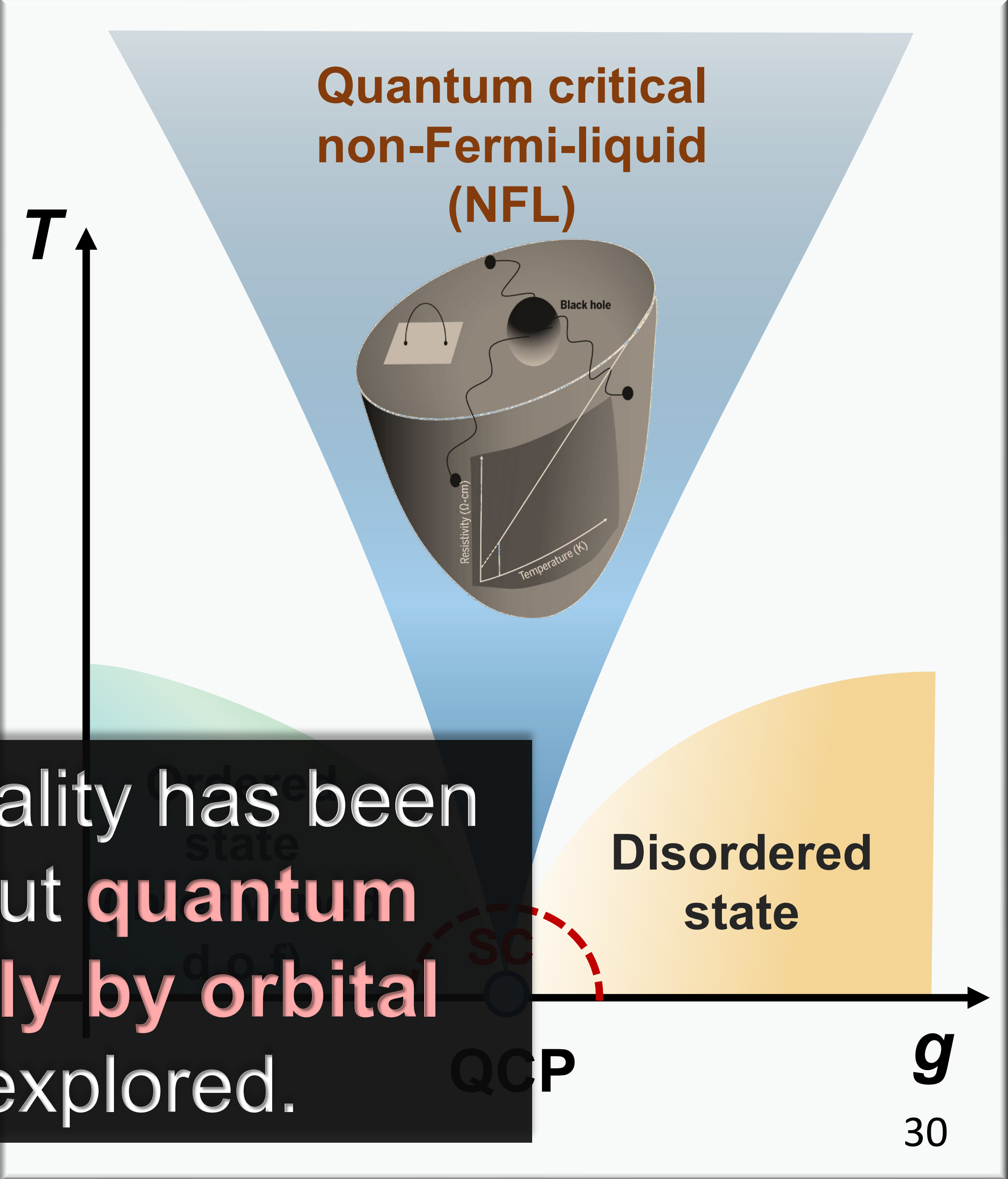

Magnetic quantum criticality has been extensively studied, but **quantum criticality driven purely by orbital fluctuations** is unexplored.

How do multipoles modify quantum phenomena?

Tuning a multipolar Kondo system to a QCP

Will the resultant phase diagram different from the Doniach phase diagram?

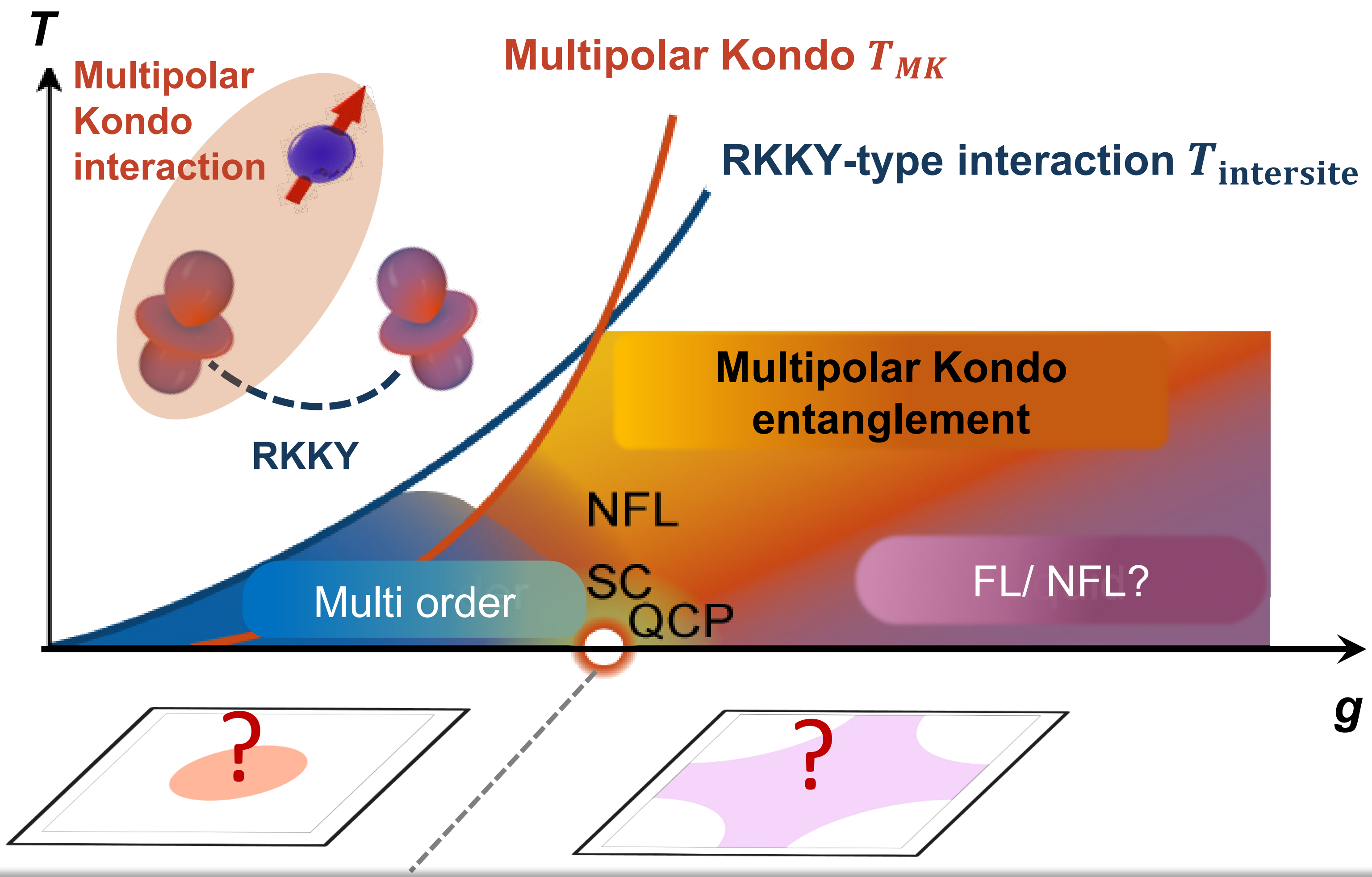

Novel quantum critical phenomena and superconductivity?

$Pr(Ti, V)_2Al_{20}$: Multipolar order, NFL, and quantum criticality

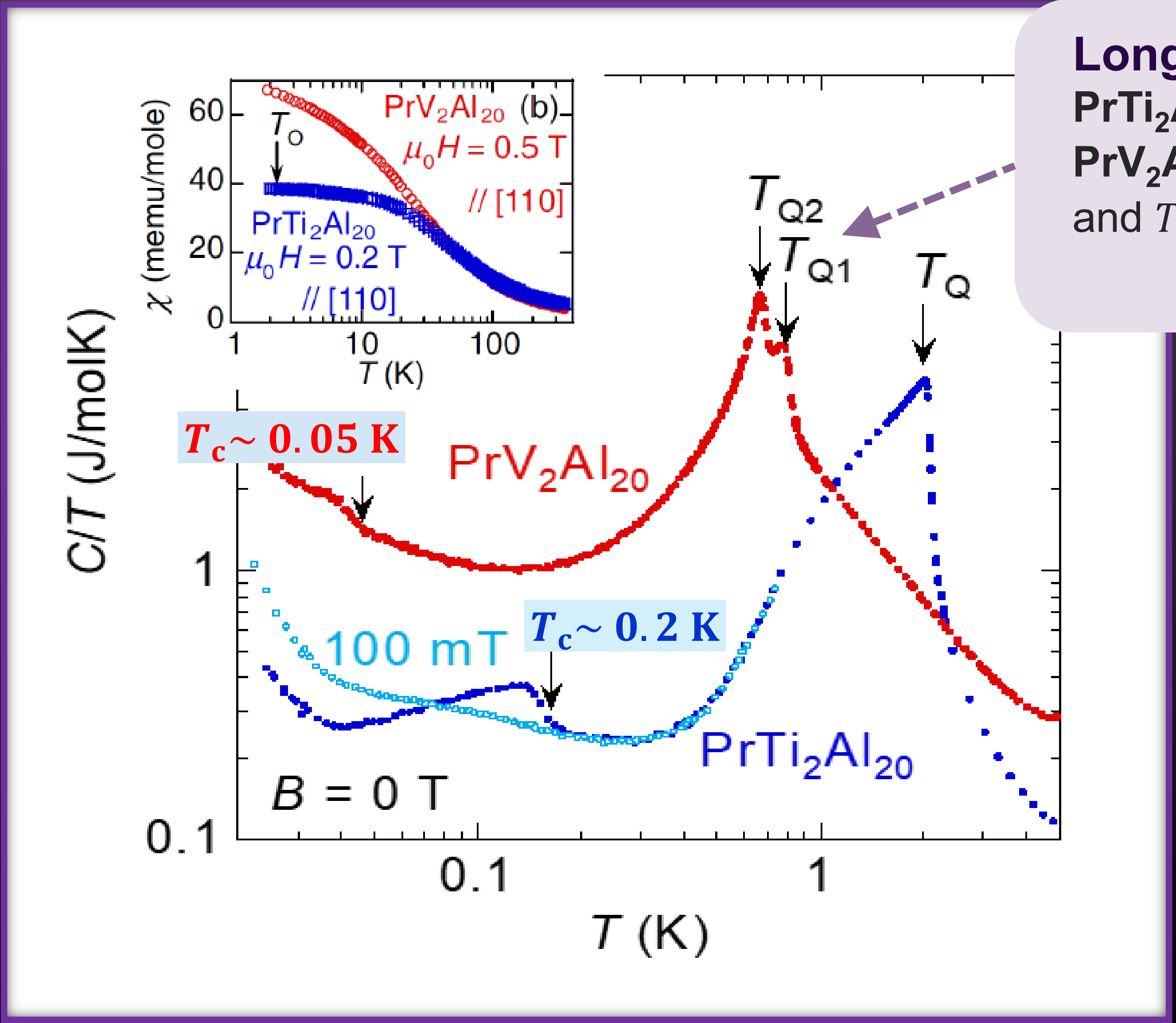

Long-range multipolar order:

$PrTi_2Al_{20}$: Ferroquadrupolar (FQ) order at $T_Q \sim 2\text{K}$

PrV_2Al_{20} : Two-stage transitions at $T_Q \sim 0.75\text{K}$ (AFQ) and $T^* \sim 0.65\text{K}$ (octupolar order?)

A. Sakai and S. Nakatsuji, JPSJ **80**, 063701 (2011)

$Pr(Ti, V)_2Al_{20}$: Multipolar order, NFL, and quantum criticality

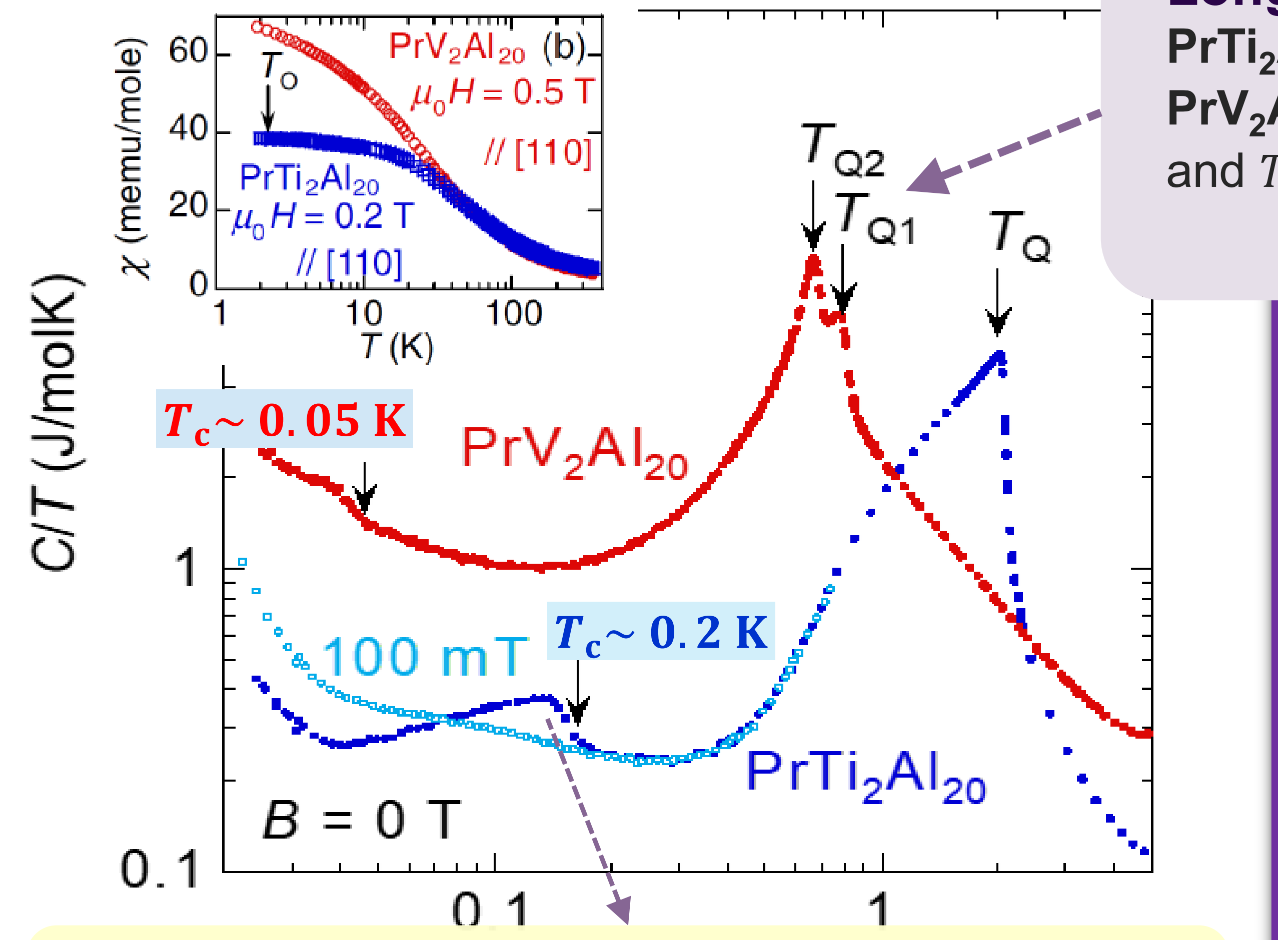

Long-range multipolar order:

$PrTi_2Al_{20}$: Ferroquadrupolar (FQ) order at $T_Q \sim 2\mathrm{K}$

PrV_2Al_{20} : Two-stage transitions at $T_Q \sim 0.75\mathrm{K}$ (AFQ) and $T^* \sim 0.65\mathrm{K}$ (octupolar order?)

A. Sakai and S. Nakatsuji, JPSJ **80**, 063701 (2011)

Heavy fermion superconductivity:

large γ and $dB_{c2}/dT\,|_{T=T_c}$ m^*/m_0 ~ 20, (Ti), 150 (V).

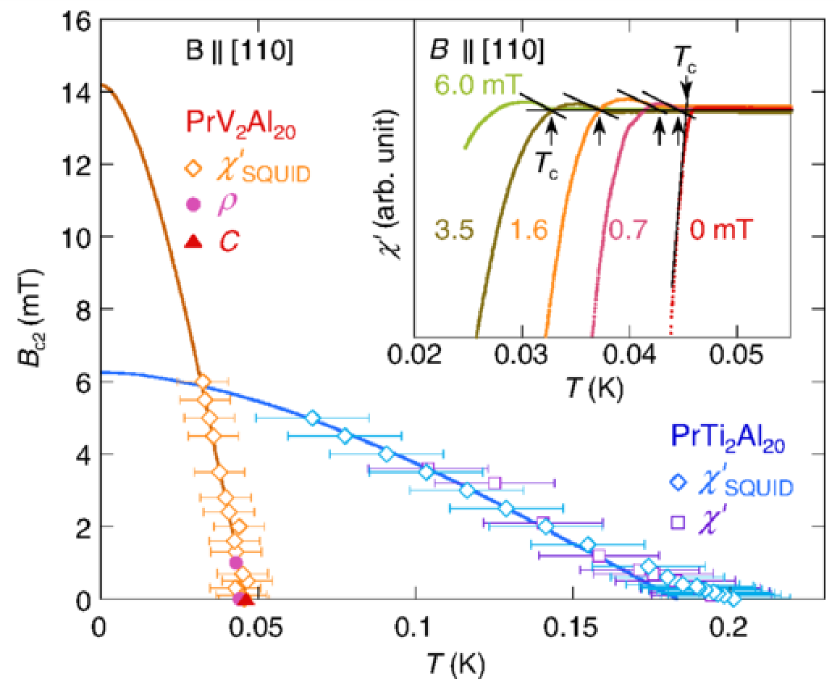

M. Tsujimoto *et al.*, PRL **113**, 267001 (2014)

$Pr(Ti, V)_2Al_{20}$: Multipolar order, NFL, and quantum criticality

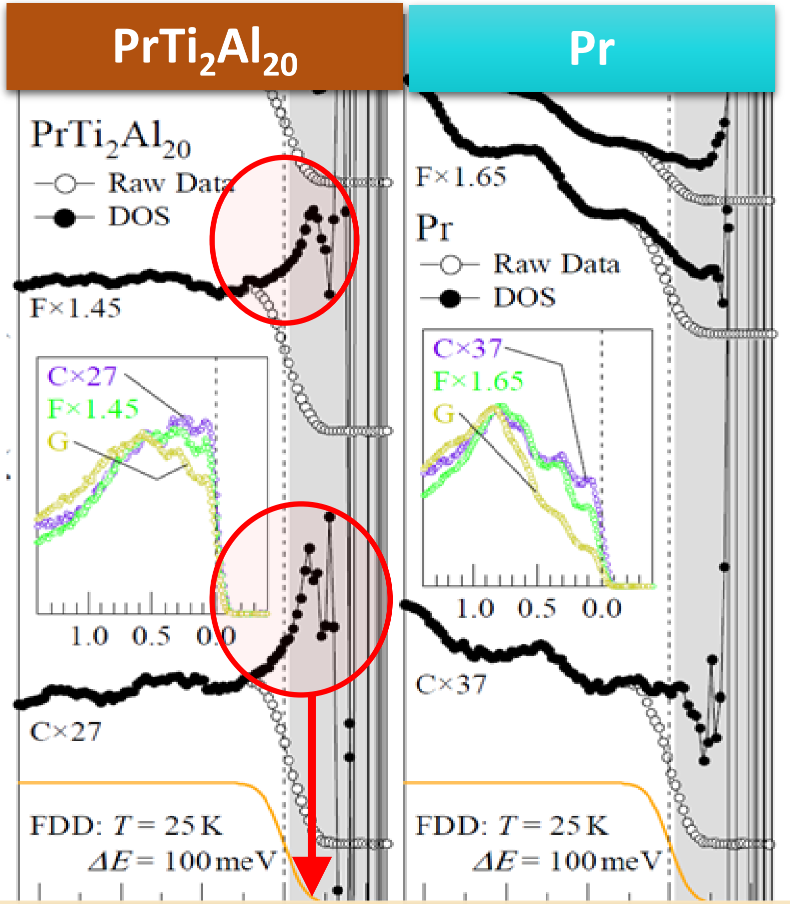

Kondo resonant peak in $PrTi_2Al_{20}$
→ substantial *c*-*f* hybridization

M. Matsunami *et al.*, PRB **84**, 193101 (2011)

Tuning chemical pressure:
Volume $PrTi_2Al_{20}$ > PrV_2Al_{20}

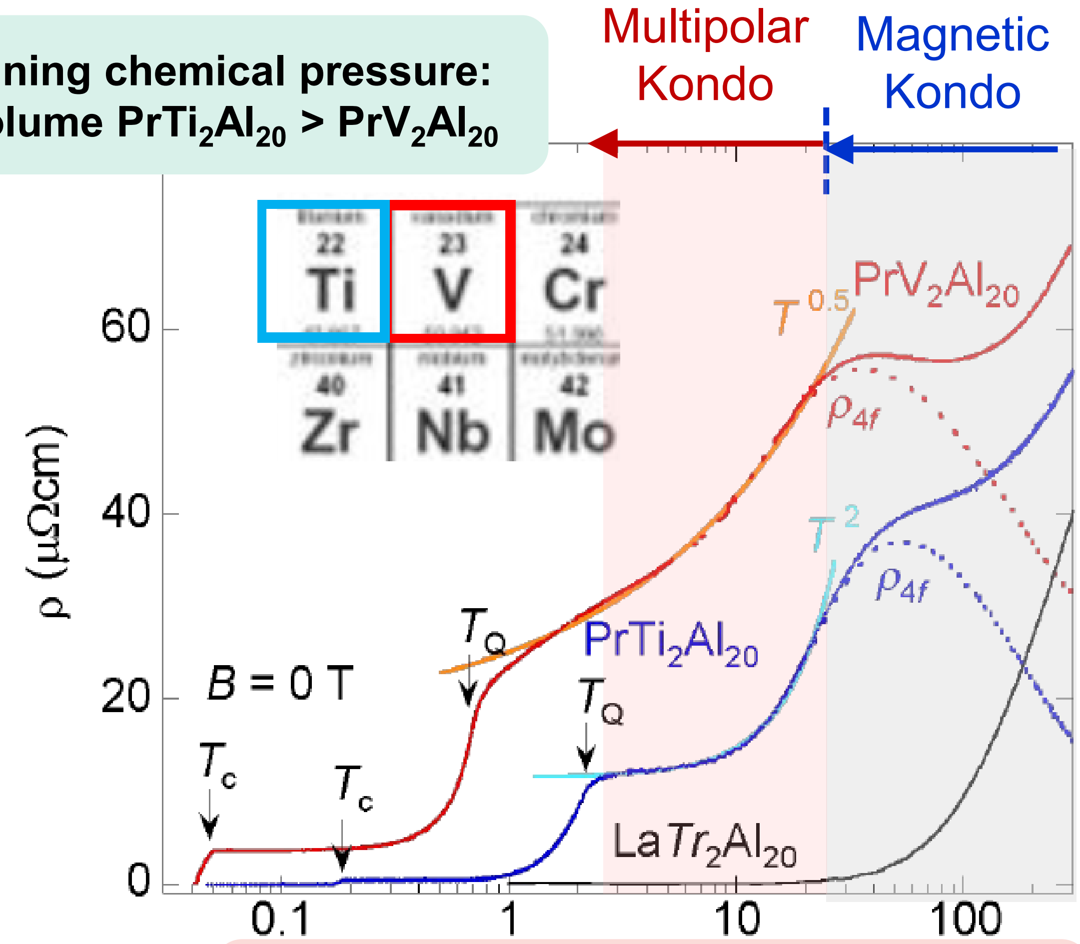

NFL behavior $\rho \sim \sqrt{T}$ in PrV_2Al_{20}
due to stronger hybridization

$Pr(Ti, V)_2Al_{20}$: Multipolar order, NFL, and quantum criticality

K. Matsubayashi *et al.*, PRL. **109**, 187004 (2012), & preprint.

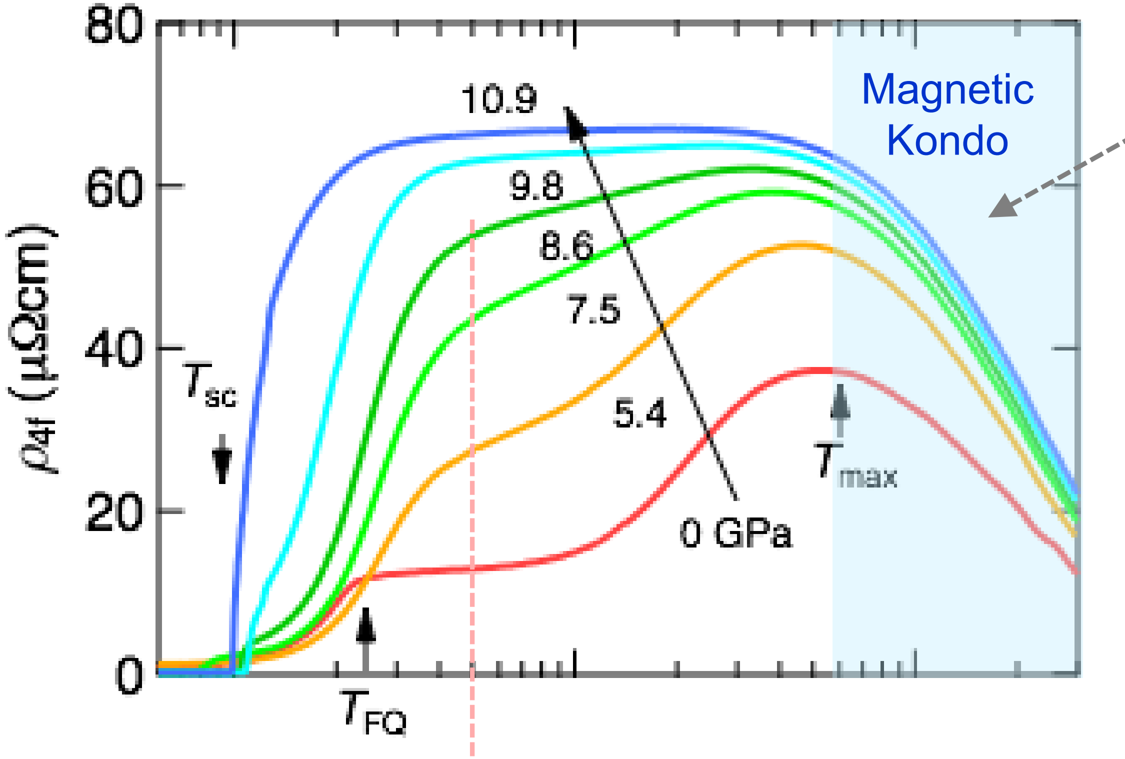

The -ln*T* behavior driven by the magnetic Kondo effect increases in magnitude → *c*-*f* hybridization enhances under pressure

Resistivity becomes incoherent near P_c~ 11 Gpa

$Pr(Ti, V)_2Al_{20}$: Multipolar order, NFL, and quantum criticality

K. Matsubayashi *et al.*, PRL. **109**, 187004 (2012), & preprint.

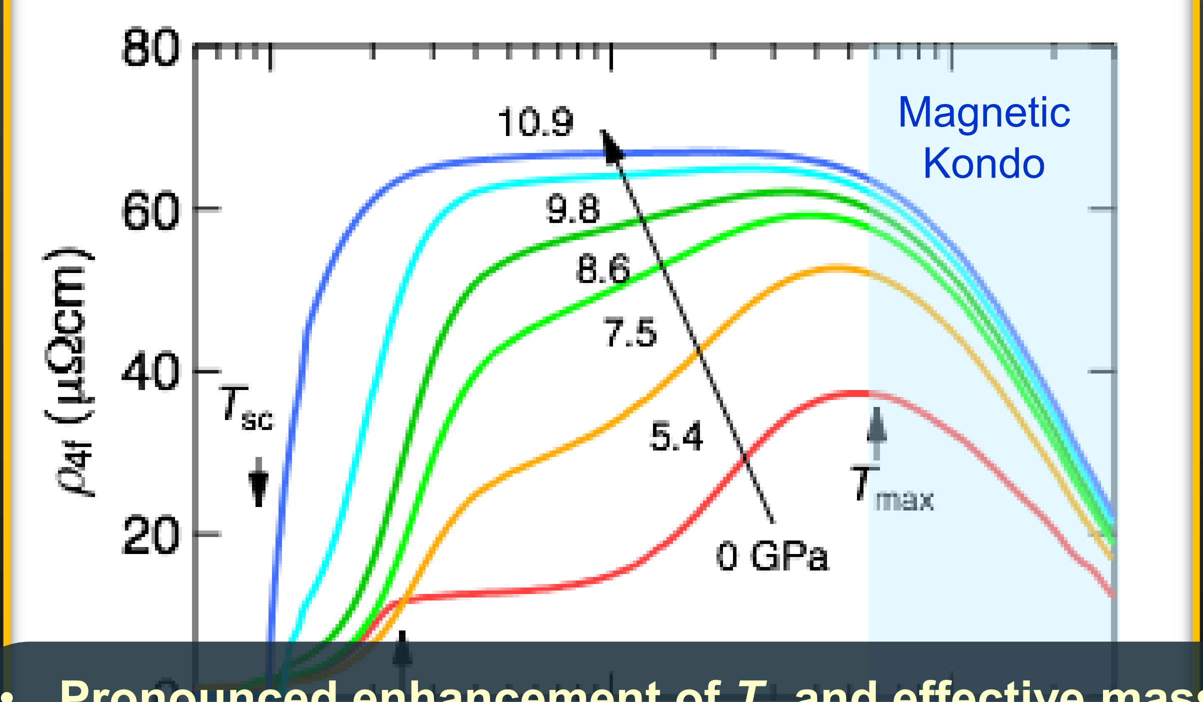

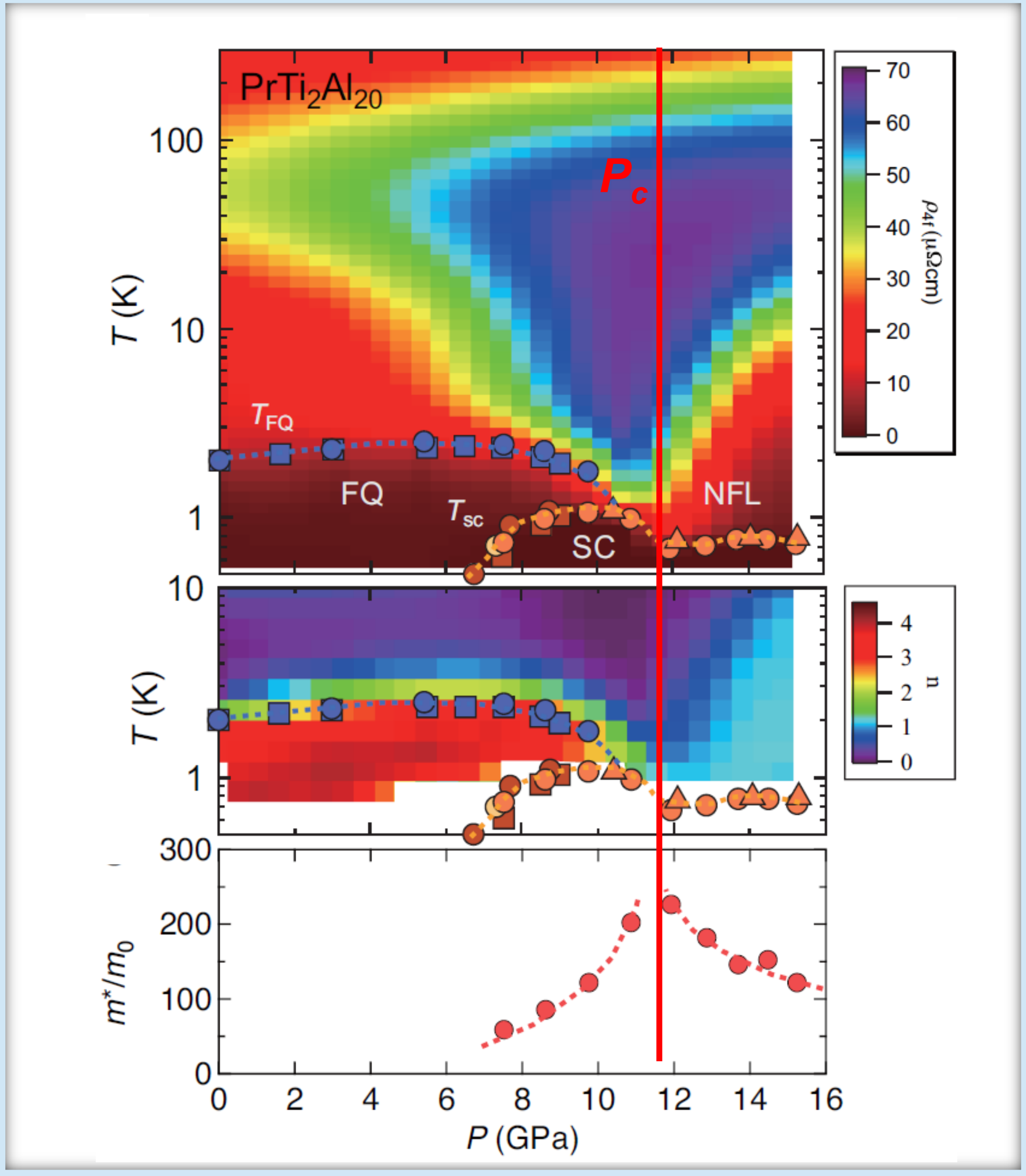

- **Pronounced enhancement of T_c and effective mass m^*** on approaching P_c ~ 11 GPa;
- **two SC domes** extending to 16 GPa
- **Robust NFL behavior** covering a wide parameter range; **FL phase does not recover under high pressures**

Topological and Multipolar Magnets and Spintronics

Satoru Nakatsuji

Dept. of Physics, University of Tokyo
Institute for Solid State Physics (ISSP), University of Tokyo
Institute of Quantum Matters (IQM), Johns Hopkins University